as reported previously[25] with 50 mM Tris-maleate buffer (pH 7.4 at 4 °C), 10–40 nM PKC C1 peptide, 20 nM [^{3}H]PDBu (16.3 Ci/mmol), 50 μg/mL 1,2-dioleoyl-*sn*-glycero-3-phospho-L-serine, 3 mg/mL bovine γ-globulin, and various concentrations of inhibitor. Binding affinity was evaluated on the basis of the concentration required to cause 50% inhibition of the specific binding of [^{3}H]PDBu, IC_{50}, which was calculated with PriProbit 1.63 software.[26] The inhibition constant K_i was calculated using the method of Sharkey and Blumberg.[24] Although we used each PKC C1 peptide in the range 10–40 nM, the concentration of the properly folded peptide was estimated to be about 3 nM based on the B_{max} values of the Scatchard analyses reported previously[25]; therefore, the concentration of free PDBu will not markedly vary over the dose–response curve.

5.6. Knockdown of XIAP using siRNA

siRNA for XIAP (HSS100565) and the control (12935-112) were purchased from Invitrogen (CA), and were transfected into cells using Lipofectamine RNAi MAX (13778150, Invitrogen). After 48 h of transfection of each siRNA, test compounds were treated, followed by cell death assay. Expression levels of XIAP and β-actin (loading control) were examined by SDS–PAGE and immunoblotting with the primary antibodies against XIAP (610762; BD Biosciences Pharmingen, CA) and β-actin (A5316; Sigma–Aldrich, MO).

5.7. Cell death assay

HeLa cells were seeded at 2×10^4 cells/well in 48-well plates and cultured overnight. The cells were treated with various concentrations of test compounds for 48 h. Cell viability was counted by trypan blue dye exclusion assay (Fig. 4A and B). HeLa cells were seeded at 1×10^5 cells/well in 12-well plates and cultured overnight. The cells were treated with various concentrations of test compounds for 24 h. Subsequently, cells were stained with propidium iodide, followed by determination of cell death by fluorescence-activated cell sorting (FACS) analysis (Epics Altra; Beckman Coulter, CA) of DNA fragmentation of propidium iodide-stained nuclei (sub-G1 population was measured) (Fig. 4C). z-VAD-fmk was purchased from Sigma–Aldrich (MO).

Acknowledgments

We are grateful to T. Watabe, Y. Fujimoto, and Y. Matsui (Keio University) for help with construction of the UNP library. This study was supported in part by a 2009 Innovative Research Program Award from the Japanese Society of Bioscience, Biotechnology, and Agrochemistry (JSBBA). T.K. was a research assistant for the Global COE Program for Human Metabolomic Systems Biology.

Supplementary data

Supplementary data associated with this article can be found, in the online version, at doi:10.1016/j.bmc.2011.05.009. These data include MOL files and InChiKeys of the most important compounds described in this article.

References and notes

1. LaCasse, E. C.; Mahoney, D. J.; Cheung, H. H.; Plenchette, S.; Baird, S.; Korneluk, R. G. *Oncogene* **2008**, *27*, 6252.
2. Deveraux, Q. L.; Takahashi, R.; Salvesen, G. S.; Reed, J. C. *Nature* **1997**, *388*, 300.
3. Deveraux, Q. L.; Roy, N.; Stennicke, H. R.; Van Arsdale, T.; Zhou, Q.; Srinivasula, S. M.; Alnemri, E. S.; Salvesen, G. S.; Reed, J. C. *EMBO J.* **1998**, *17*, 2215.
4. Deveraux, Q. L.; Leo, E.; Stennicke, H. R.; Welsh, K.; Salvesen, G. S.; Reed, J. C. *EMBO J.* **1999**, *18*, 5242.
5. Harlin, H.; Reffey, S. B.; Duckett, C. S.; Lindsten, T.; Thompson, C. B. *Mol. Cell. Biol.* **2001**, *21*, 3604.
6. Li, J. W.; Vederas, J. C. *Science* **2009**, *325*, 161.
7. Feher, M.; Schmidt, J. M. *J. Chem. Inf. Comput. Sci.* **2003**, *43*, 218.
8. Abel, U.; Koch, C.; Speitling, M.; Hansske, F. G. *Curr. Opin. Chem. Biol.* **2002**, *6*, 453.
9. Liu, X.; Ashforth, E.; Ren, B.; Song, F.; Dai, H.; Liu, M.; Wang, J.; Xie, Q.; Zhang, L. *J. Antibiot.* **2010**, *63*, 415.
10. Schimmer, A. D.; Welsh, K.; Pinilla, C.; Wang, Z.; Krajewska, M.; Bonneau, M. J.; Pedersen, I. M.; Kitada, S.; Scott, F. L.; Bailly-Maitre, B., et al *Cancer Cell* **2004**, *5*, 25.
11. Sakai, S.; Aimi, N.; Yamaguchi, K.; Hitotsuyanagi, Y.; Watanabe, C.; Yokose, K.; Koyama, Y.; Shudo, K.; Itai, A. *Chem. Pharm. Bull.* **1984**, *32*, 354.
12. Hitotsuyanagi, Y.; Fujiki, H.; Suganuma, M.; Aimi, N.; Sakai, S.; Endo, Y.; Shudo, K.; Sugimura, T. *Chem. Pharm. Bull.* **1984**, *32*, 4233.
13. Irie, K.; Isaka, T.; Iwata, Y.; Yanai, Y.; Nakamura, Y.; Koizumi, F.; Ohigashi, H.; Wender, P. A.; Satomi, Y.; Nishino, H. *J. Am. Chem. Soc.* **1996**, *118*, 10733.
14. Fujiki, H.; Suganuma, M.; Matsukura, N.; Sugimura, T.; Takayama, S. *Carcinogenesis* **1982**, *3*, 895.
15. Fujiki, H.; Sugimura, T. *Adv. Cancer Res.* **1987**, *49*, 223.
16. Irie, K.; Oie, K.; Nakahara, A.; Yanai, Y.; Ohigashi, H.; Wender, P. A.; Fukuda, H.; Konishi, H.; Kikkawa, U. *J. Am. Chem. Soc.* **1998**, *120*, 9159.
17. Hu, Y.; Cherton-Horvat, G.; Dragowska, V.; Baird, S.; Korneluk, R. G.; Durkin, J. P.; Mayer, L. D.; LaCasse, E. C. *Clin. Cancer Res.* **2003**, *9*, 2826.
18. Newman, D. J.; Cragg, G. M. *J. Nat. Prod.* **2007**, *70*, 461.
19. Weissman, K. J.; Müller, R. *Chembiochem* **2008**, *9*, 826.
20. McDaniel, R.; Thamchaipenet, A.; Gustafsson, C.; Fu, H.; Betlach, M.; Ashley, G. *Proc. Natl. Acad. Sci. U.S.A.* **1999**, *96*, 1846.
21. Murakami, H.; Ohta, A.; Ashigai, H.; Suga, H. *Nat. Methods* **2006**, *3*, 357.
22. Wu, T. Y.; Wagner, K. W.; Bursulaya, B.; Schultz, P. G.; Deveraux, Q. L. *Chem. Biol.* **2003**, *10*, 759.
23. Horiuchi, T.; Fujiki, H.; Suganuma, M.; Hakii, H.; Nakayasu, M.; Hitotsuyanagi, Y.; Aimi, N.; Sakai, S.; Endo, Y.; Shudo, K., et al *Gann* **1984**, *75*, 837.
24. Sharkey, N. A.; Blumberg, P. M. *Cancer Res.* **1985**, *45*, 19.
25. Shindo, M.; Irie, K.; Nakahara, A.; Ohigashi, H.; Konishi, H.; Kikkawa, U.; Fukuda, H.; Wender, P. A. *Bioorg. Med. Chem.* **2001**, *9*, 2073.
26. Sakuma, M. *Appl. Entomol. Zool.* **1998**, *33*, 339.
27. Raghunath, A.; Ling, M.; Larsson, C. *Biochem. J.* **2003**, *370*, 901.
28. Quest, A. F. G.; Bell, R. M. *J. Biol. Chem.* **1994**, *269*, 20000.
29. Szallasi, Z.; Bogi, K.; Gohari, S.; Biro, T.; Acs, P.; Blumberg, P. M. *J. Biol. Chem.* **1996**, *271*, 18299.
30. Masuda, A.; Irie, K.; Nakagawa, Y.; Ohigashi, H. *Biosci., Biotechnol., Biochem.* **2002**, *66*, 1615.

Biosci. Biotechnol. Biochem., **75** (2), 367–369, 2011

Note

A New, Convenient Cell-Based Screening Method for Small-Molecule Glycolytic Inhibitors

Mitsuhiro KITAGAWA,* Mayuko MISAWA, Seiichiro OGAWA, Etsu TASHIRO, and Masaya IMOTO†

Department of Biosciences and Informatics, Faculty of Science and Technology, Keio University, 3-14-1 Hiyoshi, Kohoku-ku, Yokohama, Kanagawa 223-8522, Japan

Received September 28, 2010; Accepted October 30, 2010; Online Publication, February 7, 2011
[doi:10.1271/bbb.100693]

To counteract active glycolysis in tumors, we developed a new, convenient cell-based screening system to identify an inhibitor of glycolysis. Using this system, we searched for an inhibitor in the synthetic Carbasugar library and found two candidates. It was found that both inhibited glycolysis by suppressing the glucose uptake step in tumor cells.

Key words: inhibitor screening; tumor glycolysis; glucose uptake inhibitor; carbasugar library

It is widely recognized that solid tumors exposed to hypoxia can survive and grow aggressively despite low oxygen and limited nutrition. Active glycolysis, well known as the Warburg effect, plays an important role as a lifeline for tumor survival and growth under these conditions by fueling cancer cells with ATP energy and supplying bioorganic components, such as nucleotides and fatty acids for growth.[1,2] Hence, glycolysis inhibitors are expected to be candidate drugs for tumor treatment, and hence screening research on these inhibitors has potential for cancer therapy. Many glycolytic inhibitors have been found to be inhibitors of key glycolytic enzymes,[3–5] but it is not easy to evaluate whether these glycolytic enzyme inhibitors actually modulate glycolysis in living cells. Hence, the establishment of a new cell-based screening system is required for the discovery of small, cell-permeable molecules that induce glycolysis inhibition in living cells.

Here we propose a novel cell-based screening method for glycolytic inhibitors.

Filopodia are spike-like cell membrane projections that contribute to tumor metastasis. Recently, we found that glycolytic suppression resulted in inhibition of filopodium protrusion in cancer cells only when their mitochondrial respiration was restricted.[6] This inhibition of filopodium protrusion might occur due to decreased intracellular ATP concentration caused by blocking of both glycolysis and mitochondrial respiration.[6–9] Since the test for filopodium inhibition is an easy, low-cost, quick assay, here we utilized it as a cell-based screening method for a new glycolytic inhibitor. In the assay, screening samples were added to human adenocarcinoma A431 cells co-treated with and without the mitochondrial respiratory inhibitor rotenone and

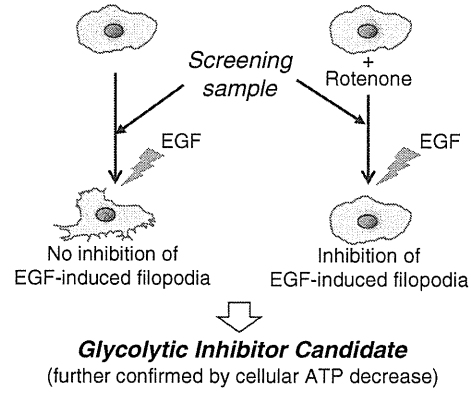

Fig. 1. Image of Screening for Glycolytic Inhibitors by EGF-Induced Filopodium Protrusion Assay.

were examined for their inhibitory effect on EGF-induced filopodium protrusion, which is easily judged by microscopic observation in 30 min (Fig. 1). A potential glycolytic inhibitor would inhibit filopodium protrusion only by co-treatment with a mitochondrial respiratory inhibitor. In the event, 2-deoxy-D-glucose (2DG), an inhibitor of glycolytic enzyme hexokinase, inhibited EGF-induced filopodium protrusion only in the presence of rotenone (Fig. 2A), indicating that this assay system works successfully. As screening source, we used a chemical library composed of 1,069 compounds, mainly cyclohexanepolyols and derivatives thereof. These compounds were carbocyclic analogs of hexopyranoses called carbasugars. The carbasugar library was originally prepared in the course of studies of the development of bioactive substances, such as antibacterial and anticancer compounds, sweeteners, and enzyme inhibitors by Ogawa *et al.* The structural features of carbasugars possibly mimic those of glucose or glycolytic metabolites, and thus are an attractive screening source for glycolytic inhibitors.

In the first screening run, 10 μg/mL of compounds (in DMSO) were tested. Hit candidates in the first run were tested again at various concentrations. We identified two compounds (sample #169 [1,4,5,6-tetra-*O*-acetyl-2-*O*-mesyl-3-*O*-benzoyl-*myo*-inositol[10]] and sample #288 [1,2,4,5-tetra-*O*-acetyl-3,6-di-*O*-tosyl-*muco*-inositol[11]]) as glycolytic inhibitors that showed filopodium inhibition only in the presence of the mitochondrial respira-

† To whom correspondence should be addressed. Fax: +81-45-566-1557; E-mail: imoto@bio.keio.ac.jp
* Present address: *Institute for Advanced Biosciences, Keio University, 246-2 Mizukami, Kakuganji, Tsuruoka, Yamagata 997-0052, Japan*
Abbreviations: EGF, epidermal growth factor; 2DG, 2-deoxy-D-glucose; RTN, rotenone

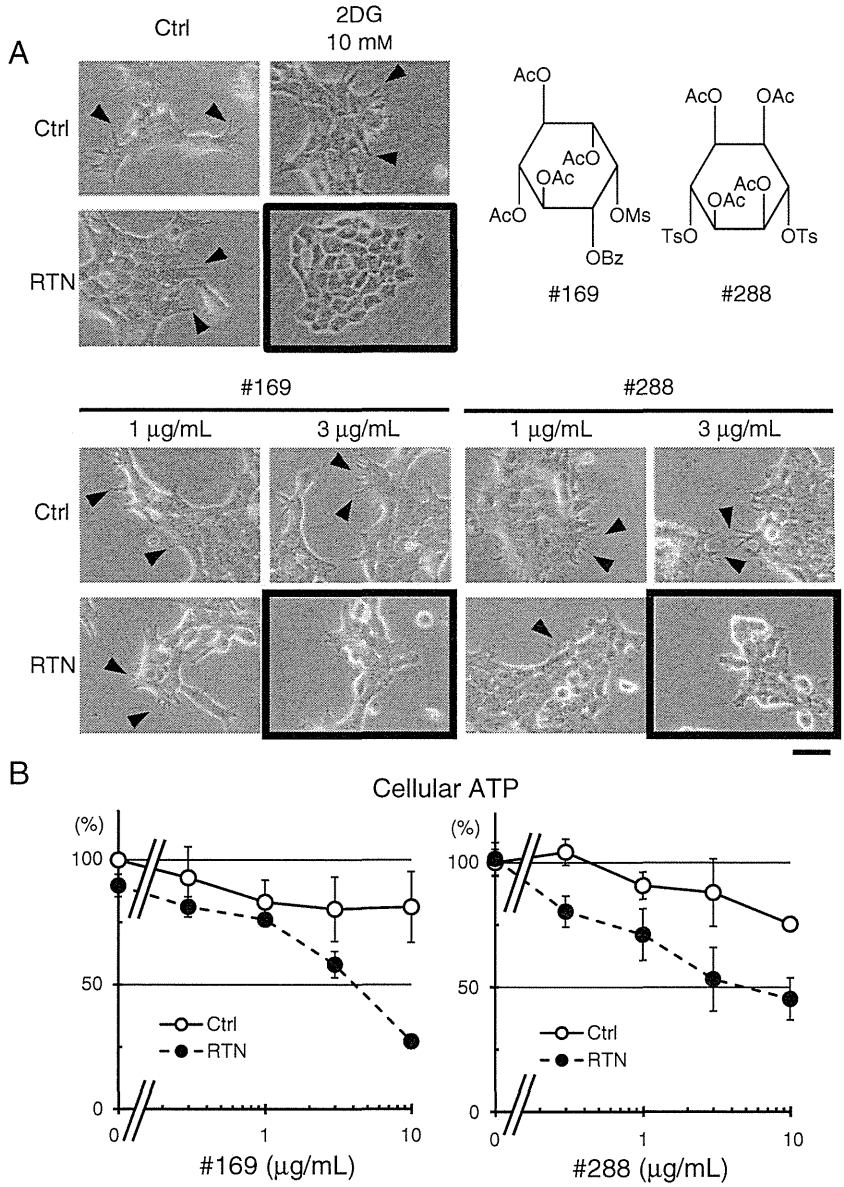

Fig. 2. Screening for Glycolytic Inhibitors in the Carbasugar Library.

A, Samples from the pseudo-sugar library were originally prepared and re-crystallized for storage by Ogawa *et al.* Two compounds, #169[10] and #288,[11] in the library, showed filopodia inhibition only in the presence of the mitochondrial respiratory inhibitor. The assay method was as described previously.[6] Hexokinase inhibitor 2-deoxyglucose (2DG, 10 mM) was used as positive control, and rotenone (RTN, 300 nM) was used to inhibit mitochondrial respiration. The arrowhead indicates filopodia, and the framed photos showed filopodium inhibition. Scale bar, 40 μm. Data represent two independent experiments. Sample purity was confirmed by LC-MS. B, Glycolytic inhibition. A431 cells were treated with the test compounds in the presence of rotenone (RTN, 300 nM) and of its solvent, ethanol, for 30 min. Cellular ATP levels were determined by luciferin-luciferase reaction (Sigma, St. Louis, MO). Bars, s.d. (n = 3). Data represent three independent experiments.

tory inhibitor rotenone (Fig. 2A). Next we tested to determine whether they would indeed suppressed glycolysis. It has been stated that glycolytic limitation caused a marked ATP decrease in tumor cells when mitochondria respiration was inhibited.[6,8] As shown in Fig. 2B, the above candidate glycolytic inhibitors slightly decreased cellular ATP in the absence of the mitochondria respiratory inhibitor. However, in combination with the mitochondria respiratory inhibitor, they did decrease intracellular ATP levels in a dose-dependent manner, indicating that they inhibited glycolysis.

To investigate further how they inhibit glycolysis, we examined their effects on the 3 steps of glycolysis: glucose uptake, hexokinase, and pyruvate kinase. It has been reported that these steps play important roles in accelerated glycolysis in tumor metabolism, and higher expression levels of the proteins facilitating these steps are frequently observed.[3,12–14] Neither #169 nor #288 affected hexokinase or pyruvate kinase reactions at up to 30 μg/mL (Fig. 3A), but they inhibited the glucose uptake step dose-dependently, with IC_{50} values of 4.5 μg/mL for #169 and 2.7 μg/mL for #288 (Fig. 3B). Inhibition of glucose uptake was similar to that due to decreasing intracellular ATP levels in the presence of rotenone, as shown in Fig. 2B, suggesting that both #169 and #288 suppressed glycolysis by inhibiting cellular glucose uptake.

In summary, here we propose a new, convenient screening assay for glycolytic inhibitors. We found two glycolytic inhibitors in a carbasugar library. They limited glycolysis by inhibiting glucose uptake at several μg/mL concentrations.

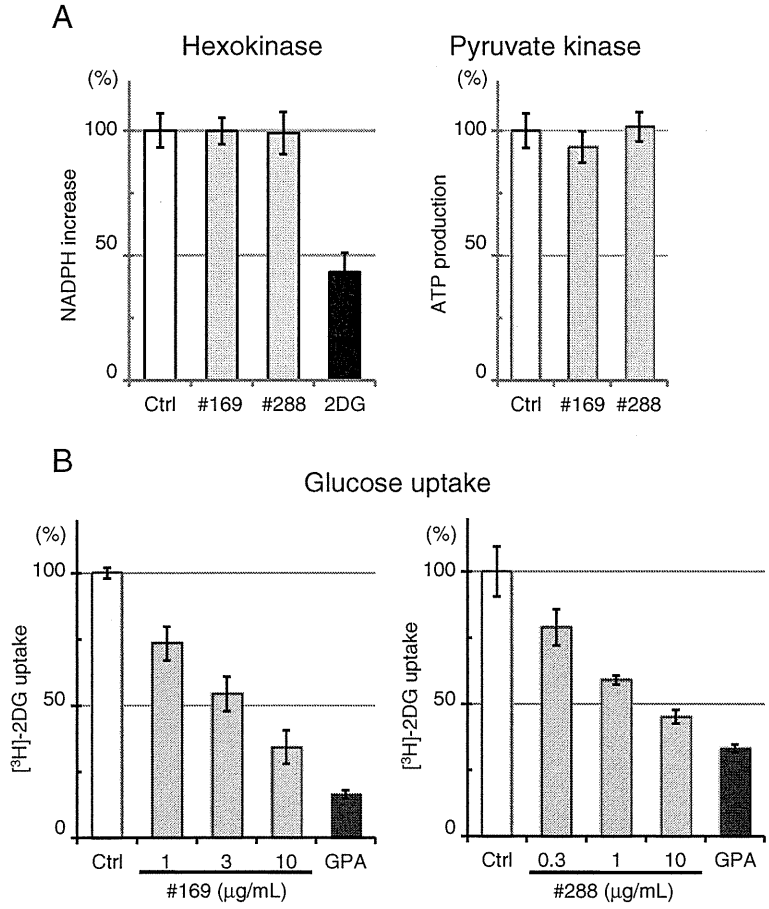

Fig. 3. Inhibition of the Glucose Uptake Step to Explain Glycolytic Suppression by #169 and #288.

A, Effects of compounds on the activities of two of the rate-limiting enzymes *in vitro*. Hexokinase activity was determined as described previously.[6] For pyruvate kinase activity, purified recombinant human pyruvate kinase 1 was used. The complete human pyruvate kinase 1 from HeLa cDNA was cloned into *E. coli* expression vector pRSETc. The reaction (3 μM ADP and 0.3 μM F1, 6P for the substrate in PK buffer, containing 5 mM $MgCl_2$, 0.1 mg/mL BSA, 2 mM DTT, 1 mM EDTA, 50 mM KCl, 50 mM Tris pH 7.7) for 30 min was quenched with TCA and neutralized. Enzymatic activity was calculated by ATP production. Bars, s.d. (n = 3). B, Inhibition of glucose uptake by #169 and #288. The assay method was as described previously,[6] and glucopiericidin A (GPA, 10 ng/mL) was used as positive control.[6] Bars, s.d. (n = 3). Data represent three independent experiments.

Further studies of structural modification to develop more potent inhibitors and analysis of structure-activity relationships are now under investigation.

Acknowledgments

This work was supported by a grant from the Ministry of Education, Culture, Sports, Science, and Technology of Japan.

References

1) Deberardinis RJ, Mancuso A, Daikhin E, Nissim I, Yudkoff M, Wehrli S, and Thompson CB, *Proc. Natl. Acad. Sci. USA*, **104**, 19345–19350 (2007).
2) Hsu PP and Sabatini DM, *Cell*, **134**, 703–707 (2008).
3) Madhok BM, Yeluri S, Perry SL, Hughes TA, and Jayne DG, *Am. J. Clin. Oncol.*, in press.
4) Shanmugam M, Mcbrayer SK, and Rosen ST, *Curr. Opin. Oncol.*, **21**, 531–536 (2009).
5) Vander Heiden MG, Christofk HR, Schuman E, Subtelny AO, Sharfi H, Harlow EE, Xian J, and Cantley LC, *Biochem. Pharmacol.*, **79**, 1118–1124 (2010).
6) Kitagawa M, Ikeda S, Tashiro E, Soga T, and Imoto M, *Chem. Biol.*, **17**, 989–998 (2010).
7) Le Clainche C and Carlier M-F, *Physiol. Rev.*, **88**, 489–513 (2008).
8) Molitoris BA, Geerdes A, and Mcintosh JR, *J. Clin. Invest.*, **88**, 462–469 (1991).
9) Witke W, *Trends Cell Biol.*, **14**, 461–469 (2004).
10) Suami T, Lichtenthaler F, and Ogawa S, *Bull. Chem. Soc. Jpn.*, **39**, 170–178 (1966).
11) Ogawa S, Oki S, and Suami T, *Bull. Chem. Soc. Jpn.*, **52**, 1095–1101 (1979).
12) Airley RE and Mobasheri A, *Chemotherapy*, **53**, 233–256 (2007).
13) Mathupala SP, Ko YH, and Pedersen PL, *Oncogene*, **25**, 4777–4786 (2006).
14) Mazurek S, Boschek CB, Hugo F, and Eigenbrodt E, *Semin. Cancer Biol.*, **15**, 300–308 (2005).

Biosci. Biotechnol. Biochem., **75** (2), 284–288, 2011

Quinotrierixin Inhibited ER Stress-Induced XBP1 mRNA Splicing through Inhibition of Protein Synthesis

Kohta YAMAMOTO,† Etsu TASHIRO, and Masaya IMOTO

Department of Biosciences and Informatics, Faculty of Science and Technology, Keio University, 3-14-1 Hiyoshi, Kohoku-ku, Yokohama 223-8522, Japan

Received August 25, 2010; Accepted November 22, 2010; Online Publication, February 7, 2011
[doi:10.1271/bbb.100622]

Quinotrierixin was isolated from microbes as an inhibitor of ER stress-induced XBP1 mRNA splicing, but its mode of action was unclear. We found that quinotrierixin is an inhibitor of protein synthesis, and that the required dose range of quinotrierixin to inhibit ER stress-induced XBP1 mRNA splicing was similar to that to inhibit protein synthesis. Furthermore, we also found that quinotrierixin inhibited the ER stress-induced increases of unfolded protein response-related genes such as GRP78, CHOP, EDEM, ERdj4, and p58^{IPK}. Thus, we showed that quinotrierixin inhibited the ER stress-induced unfolded protein response, possibly due to its inhibitory activity of protein synthesis.

Key words: quinotrierixin; ER stress; XBP1; protein synthesis inhibitor

Newly synthesized polypeptides that are secreted or localized in the plasma membrane are post- or co-translationally translocated into the lumen of the endoplasmic reticulum (ER), where they are modified, folded, and assembled correctly prior to transport to the Golgi apparatus. However, when cells are faced with cytotoxic conditions, such as hypoxia and nutrient deprivation, these folding reactions are compromised and protein aggregation occurs. The unfolded proteins are retained in the ER, and the accumulation of unfolded proteins causes ER stress.[1] As a consequence, the cell activates adaptive signaling pathways that are programmed to enhance folding capabilities and to limit the folding load on the ER. This response is called the unfolded protein response (UPR).

In mammalian cells, UPR is regulated in part by ER membrane-localized IRE1α.[2–4] IRE1α induces unconventional X-box binding protein 1 (XBP1) mRNA splicing. Twenty-six nts of XBP1 mRNA are spliced out to lead the shift in the open reading frame. Translation of spliced XBP1 mRNA produces a potent transcription factor called XBP1s (the "s" indicates spliced).[5,6] XBP1s upregulates gene expression that enhances ER protein folding capacity and quality control.[7] Furthermore, it has been reported that there is a link between XBP1 and human disease, including solid tumor and inflammatory bowel disease.[8–14] Therefore, small molecule inhibitors of ER stress-induced XBP1 mRNA splicing would be very useful in fundamental research into UPR signaling, and might eventually find clinical application.

In a previous study, we established a screening system to identify small molecule inhibitors of XBP1 mRNA splicing. We have also reported that novel trieneansamycin group compounds, quinotrierixin and trierixin, inhibited ER stress-induced XBP1 mRNA splicing in HeLa cells.[15–18] In this study, we found that quinotrierixin inhibited protein synthesis. Moreover, we investigated the relationship between quinotrierixin-inhibited ER stress-induced XBP1 mRNA splicing and protein synthesis.

Materials and Methods

Materials. Quinotrierixin, trierixin, and trienomycin A were prepared as described in our previous reports.[15,17] Cytotrienin A was kindly provided by Dr. H. Osada (RIKEN, Japan). Cycloheximide, anisomycin, and puromycin were purchased from Sigma (St. Louis, MO).

Cell culture. Human epithelial adenocarcinoma cell line HeLa was cultured in DMEM supplemented with 8% FBS.

RT-PCR analysis (XBP1 mRNA splicing assay). As reported previously,[15] HeLa cells were seeded in 12-well plates at 5×10^4 cells/well, and then incubated with 10 μg/mL of tunicamycin with and without quinotrierixin and other protein synthesis inhibitors for 4 h. Subsequently, total RNA was extracted from the HeLa cells using TRIzol reagent (Invitrogen, Carlsbad, CA). Aliquots of 2.0 μg of the total RNA were treated with M-MLV reverse transcriptase (Promega, Madison, WI) to produce first-strand cDNA, which was subjected to polymerase chain reaction (PCR) with KOD plus polymerase (Toyobo, Osaka, Japan) using a pair of primers corresponding to nucleotides 505–524 and 609–629 of XBP1 cDNA. The amplified products were separated by electrophoresis on a 8% polyacrylamide gel and visualized by ethidium bromide staining.

Real-time RT-PCR. Real-time reverse transcription (RT)–polymerase chain reaction (PCR) was performed using SYBR Premix Ex Taq (Takara, Siga, Japan). The primer set was as follows: for GRP78, forward 5′-GCTCGACTCGAATTCCAAAG-3′ and reverse 5′-GATCACCAGAGAGCACACCA-3′; for CHOP, forward 5′-GCGCATGAAGGAGAAAGAAC-3′ and reverse 5′-TCACCATTCGGTCAATCAGA-3′; for ERdj4, forward 5′-AAAATAAGAGCCCGGATGCT-3′ and reverse 5′-CGCTTCTTGGATCCAGTGTT-3′; for EDEM, forward 5′-TGGACTGCAGGTGCTGATAG-3′ and reverse 5′-GGATTCTTGGTTGCCTGGTA-3′; for P58^{IPK}, forward 5′-CTCAGTTTCATGCTGCCGTA-3′ and reverse 5′-TTGCTGCAGTGAAGTCCATC-3′; and for GAPDH, forward 5′-AGGTCGGAGTCAACGGATTT-3′ and reverse 5′-TAGTTGAGGTCAATGAAGGG-3′.

Measurement of macromolecular synthesis. HeLa cells were seeded in 24-well plates at 5×10^4 cells/well and cultured overnight. Each culture well was refilled with fresh Dulbecco's Modified Eagle's

† To whom correspondence should be addressed. Tel: +81-45-566-1793; Fax: +81-45-566-1557; E-mail: tashiro@bio.keio.ac.jp

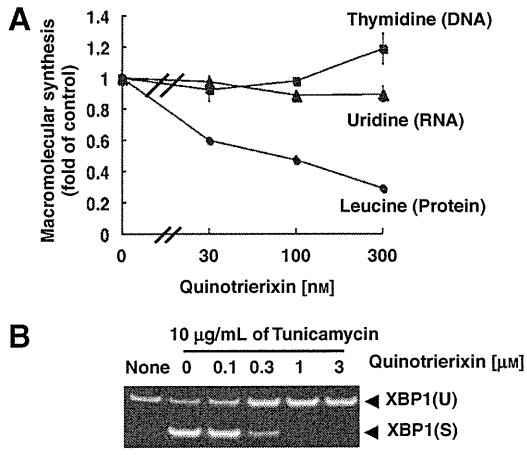

Fig. 1. Quinotrierixin, Cycloheximide, and Anisomycin Inhibited ER Stress-Induced XBP1 mRNA Splicing and Protein Synthesis.

A, Quinotrierixin inhibited protein synthesis in HeLa cells. HeLa cells were treated with the indicated concentrations of qunotrierixin with [^{3}H]-leucine, [^{3}H]-thymidine, or [^{3}H]-uridine for 1 h. The radioactivity of the macromolecular fraction was measured with a liquid scintillation counter. The representative data are the means for three independent studies. B, Quinotrierixin inhibited tunicamycin-induced XBP1 mRNA splicing. HeLa cells were treated with 10 μg/mL of tunicamycin with and without the indicated concentrations of quinotrierixin for 4 h. The cells were collected and extracted RNA was subjected to RT-PCR. Spliced and unspliced XBP1 mRNA was detected as described in "Materials and Methods." XBP1(U) and XBP1(S) indicate unspliced and spliced XBP1 mRNA respectively.

Medium (DMEM) containing 0.2% fetal bovine serum (FBS). For measurement of protein synthesis, cells were treated with 2 μCi [^{3}H]-leucine, 0.5 μCi [^{3}H]-thymidine or 0.5 μCi [^{3}H]-uridine, radioactive protein, and DNA or RNA synthesis precursor, with and without the indicated compounds for 1 h at 37 °C. After incubation, the medium was removed and the macromolecular fraction was fixed with ice-cold 10% trichloroacetic acid (TCA). Each well was washed with ice-cold 10% TCA twice, and 0.5 N NaOH was added. Radioactivity was measured with a liquid scintillation counter.

Data analysis. For determination of IC_{50} values against tunicamycin-induced XBP1 mRNA splicing, the spliced-XBP1 mRNA bands visualized with ethidium bromide staining were quantified by densitometry. IC_{50} values were determined from the dose-response curves of the inhibition of XBP1 mRNA splicing activity, where the intensity of spliced-XBP1 mRNA bands of tunicamycin treatment was defined as 100%.

IC_{50} values against protein synthesis were determined from dose-response curves, the radioactivity of non-treatment control was defined as 100%.

Real-time RT-PCR data were analyzed by paired *t*-tests to evaluate differences in means among three independent experiments, $^*p < 0.05$ and $^{**}p < 0.01$.

Results

Quinotrierixin inhibited XBP1 mRNA splicing and protein synthesis

Quinotrierixin was identified as an inhibitor of ER stress-induced XBP1 mRNA splicing, but its mode of action was unclear. Previously, cycloheximide, a well-known protein synthesis inhibitor, was reported to inhibit ER stress-induced XBP1 mRNA splicing.[19] Hence, we examined whether quinotrierixin would inhibit protein synthesis. As shown in Fig. 1A, quinotrierixin inhibited [^{3}H]-leucine uptake into the macromolecular fraction of HeLa cells in a dose-dependent manner. On the other hand, neither [^{3}H]-thymidine uptake nor [^{3}H]-uridine uptake was inhibited by quinotrierixin at up to 300 nm. These results indicate that quinotrierixin inhibits protein synthesis without affecting DNA or RNA synthesis (Fig. 1A). Because the dose range of quinotrierixin for inhibiting protein synthesis was similar to that for inhibiting tunicamycin and 2-deoxyglucose (2DG), both of which are known as ER stress inducers, -induced XBP1 mRNA splicing (Fig. 1B and Supplemental Fig. 1; see *Biosci. Biotechnol. Biochem.* Web site), another three triene-ansamycin group compounds, which inhibited ER stress-induced XBP1 mRNA splicing, were assessed for their ability to inhibit protein synthesis. As shown in Table 1, trierixin, trienomycin A, and cytotrienin A inhibited protein synthesis at almost the same concentration as for the inhibition of tunicamycin-induced XBP1 mRNA splicing.

Table 1. Inhibitory Activities of Triene-Ansamycin Group Compounds, Cycloheximide, Anisomycin, and Puromycin against ER Stress-Induced XBP1 Activation and Protein Synthesis

	XBP1 inhibition IC_{50} value [nM]	Protein synthesis inhibition IC_{50} value [nM]
Quinotrierixin	85	120
Trierixin	17	55
Trienomycin A	47	38
Cytotrienin A	190	160
Cycloheximide	530	680
Anisomycin	240	120
Puromycin	>20,000	4,400

Quinotrierixin inhibited unfolded protein response

Next, to determine whether quinotrierixin would affect other ER stress-induced unfolded protein responses, we evaluated the effects of quinotrierixin on the mRNA levels of UPR related genes, GRP78, CHOP, EDEM, ERdj4, and p58^{IPK}, under ER stress conditions. We found that quinotrierixin completely suppressed the increases in GRP78, CHOP, EDEM, ERdj4, and p58^{IPK} mRNA induced by tunicamycin or 2DG at the same concentration as for inhibition of protein synthesis and XBP1 mRNA splicing. (Fig. 2 and Supplemental Fig. 2). These results indicate that quinotrierixin did not specifically inhibit ER stress-induced XBP1 mRNA splicing, but rather that quinotrierixin would induce the shutdown of all ER stress-induced UPR.

Cycloheximide and anisomycin, but not puromycin, inhibited the unfolded protein response

To confirm that protein synthesis inhibition due to quinotrierixin results in the suppression of ER stress-induced UPR, we determined whether other protein synthesis inhibitors would inhibit ER stress-induced UPR. As shown in Figs. 3A and 4 and Supplemental Figs. 1 and 2, anisomycin as well as cycloheximide inhibited not only XBP1 mRNA splicing but also the UPR gene upregulation induced by tunicamycin and by 2DG. On the other hand, puromycin failed to inhibit the XBP1 mRNA splicing induced by tunicamycin and by 2DG under conditions in which puromycin inhibited protein synthesis, as judged by [^{3}H]-leucine uptake into the macromolecular fraction of the HeLa cells (Table 1,

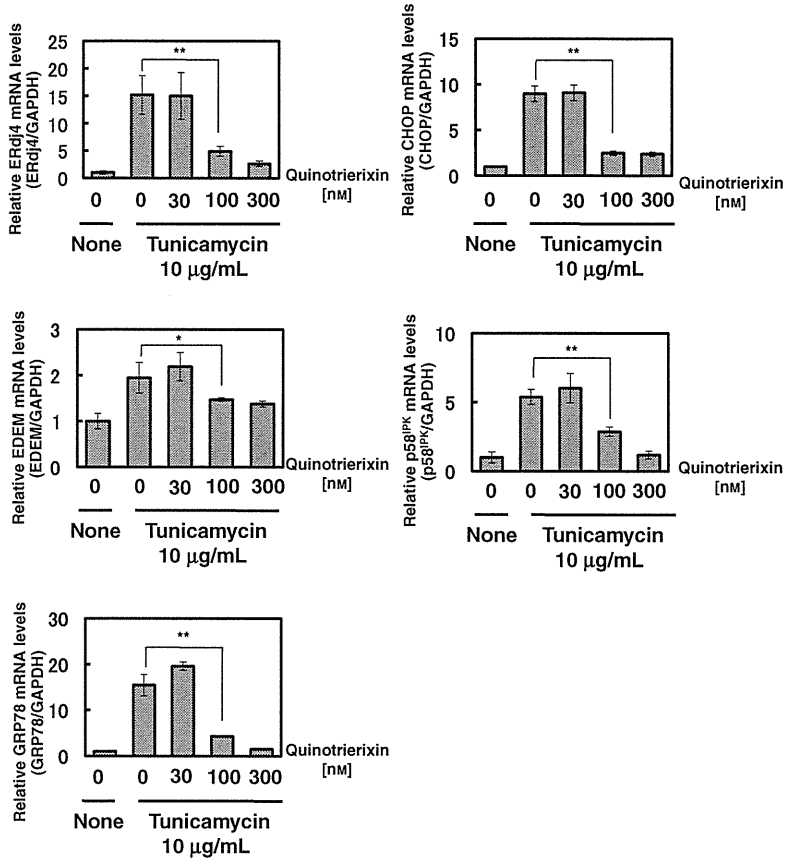

Fig. 2. Quinotrierixin Inhibited the Unfolded Protein Response.

Quinotrierixin suppressed tunicamycin-increased ERdj4, EDEM, GRP78, CHOP, and $p58^{IPK}$ mRNA. HeLa cells were treated with 10 μg/mL of tunicamycin with and without the indicated concentrations of quinotrierixin for 8 h. The cells were collected and RNA was extracted. ERdj4, EDEM, GRP78, CHOP, and $p58^{IPK}$ mRNA levels were evaluated by real-time RT-PCR. Each mRNA was normalized with the mRNA levels of GAPDH. Data are the means ± SD among three independent experiments, $^{*}p < 0.05$ and $^{**}p < 0.01$.

Fig. 3A, and Supplemental Fig. 3). Rather, consistently with a previous report,[20] single treatment of cells with puromycin induced XBP1 mRNA splicing (Fig. 3B). Both spliced and unspliced XBP1 mRNA were weakly reduced when the cells were treated with puromycin together with tunicamycin, but this was probably due to cytotoxicity, because puromycin induced cell membrane disruption at 6 μM after 4 h of treatment with puromycin together with tunicamycin (data not shown).

Discussion

In this study, we found for the first time that triene-ansamycin group compounds, including quinotrierixin, inhibited protein synthesis. Although several biological activities of triene-ansamycin antibiotics have been reported, the activity of protein synthesis inhibition has not been reported. This finding raises the possibility that some biological activities of triene-ansamycin group compounds, such as apoptosis induction,[21] inhibition of NO production,[22] and inhibition of osteoblastic resorption,[23] can be explained by inhibitory activity of protein synthesis.

Quinotrierixin and other protein synthesis inhibitors suppressed not only ER stress-induced XBP1 mRNA splicing but also other UPR, such as transcription of the UPR genes GRP78, CHOP, EDEM, ERdj4, and $p58^{IPK}$, at the same concentration as for inhibition of protein synthesis. The only exception was puromycin, which did

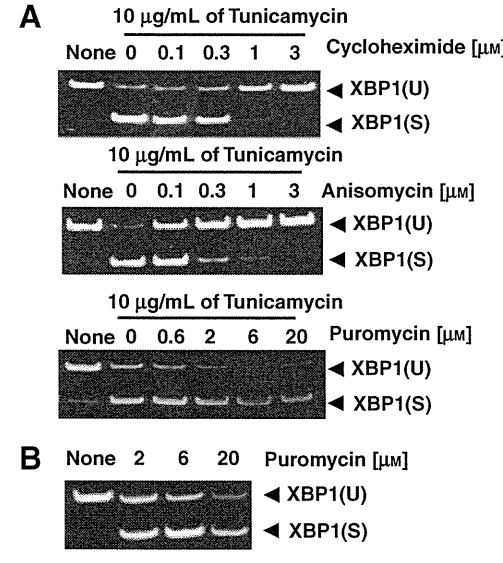

Fig. 3. Cycloheximide and Anisomycin, but Not Puromycin, Inhibited XBP1 mRNA Splicing.

A, Cycloheximide and anisomycin but not puromycin inhibited tunicamycin-induced XBP1 mRNA splicing. HeLa cells were treated with 10 μg/mL of tunicamycin with and without the indicated concentrations of cycloheximide, anisomycin, or puromycin for 4 h. B, Puromycin induced XBP1 mRNA splicing. HeLa cells were treated with the indicated concentrations of puromycin for 4 h. The cells were collected, and extracted RNA was subjected to RT-PCR. Spliced and unspliced XBP1 mRNA was detected as described in "Materials and Methods." XBP1(U) and XBP1(S) indicate unspliced and spliced XBP1 mRNA respectively.

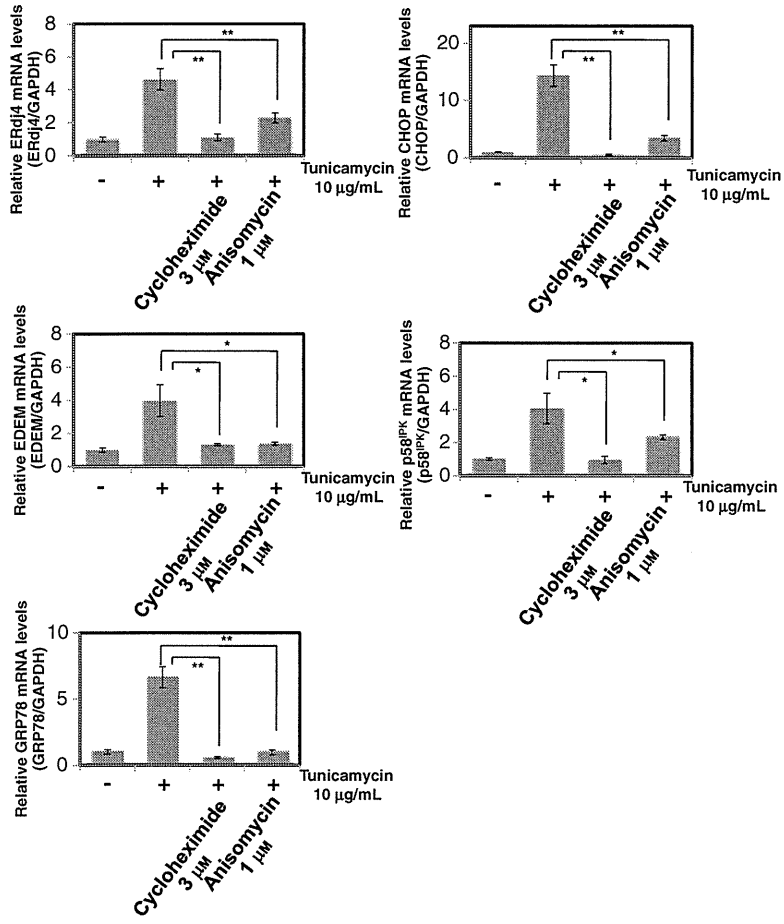

Fig. 4. Cycloheximide and Anisomycin Inhibited the Unfolded Protein Response.

Cycloheximide and anisomycin suppressed tunicamycin-increased ERdj4, EDEM, GRP78, CHOP, and $p58^{IPK}$ mRNA. HeLa cells were treated with 10 μg/mL of tunicamycin with and without the indicated concentrations of cycloheximide or anisomycin for 8 h. Cells were collected and RNA was extracted. ERdj4, EDEM, GRP78, CHOP, and $p58^{IPK}$ mRNA levels were evaluated by real-time RT-PCR. Each mRNA was normalized with the mRNA levels of GAPDH. Data are the means ± SD among three independent experiments, $^{*}p < 0.05$ and $^{**}p < 0.01$.

not inhibit ER stress-induced XBP1 mRNA splicing. As previously reported, puromycin alone induced UPR in HeLa cells. Hence a different effect on UPR by protein synthesis inhibitor appears to be dependent on the inhibitory mechanism of the protein synthesis inhibitor. Puromycin has been reported to enforce nascent polypeptides to release from the ribosome halfway through the elongation reaction.[24] Thus, un-maturated proteins might influx into the ER and accumulate, and then induce ER stress as unfolded proteins. In contrast, cycloheximide and anisomycin inhibited polypeptide release from the ribosomes due to inhibition of ribosome translocation and to inhibition of peptidyl transfer respectively.[25] This indicates that un-maturated proteins produced by cycloheximide or anisomycin cannot move to the ER, and fail to induce ER stress. This inhibitory mechanism of cycloheximide and anisomycin may explain why they suppress ER stress-induced UPR. These compounds prevent further influx of newly synthesized proteins into the ER, which results in a reduction in ER stress.

At present, the inhibitory mechanism in protein synthesis due to quinotrierixin remains unclear. However, because quinotrierixin suppressed ER stress-induced UPR as did cycloheximide and anisomycin but not puromycin, the mode of action of quinotrierixin would be similar to cycloheximide and anisomycin. Thus, it is likely that quinotrierixin blocked polypeptide release from the ribosomes. But further study is needed to elucidate the mechanism.

Acknowledgments

We thank Dr. Hiroyuki Osada (RIKEN, Japan) for kindly providing us with cytotrienin A. This study was partly supported by grants from Takeda Science Foundation and Suzuken Memorial Foundation. This work was also supported by a Grant-in-Aid for Scientific Research from the Ministry of Education, Culture, Sports, Science, and Technology of Japan. This study was supported in part by the Global COE Program for Human Metabolomic Systems Biology of MEXT, Japan.

References

1) Ellgaard L and Helenius A, *Curr. Opin. Cell Biol.*, **13**, 431–437 (2001).
2) Zhou J, Liu CY, Back SH, Clark RL, Peisach D, Xu Z, and Kaufman RJ, *Proc. Natl. Acad. Sci. USA*, **103**, 14343–14348 (2006).
3) Wang XZ, Harding HP, Zhang Y, Jolicoeur EM, Kuroda M, and Ron D, *EMBO J.*, **17**, 5708–5717 (1998).
4) Credle JJ, Finer-Moore JS, Papa FR, Stroud RM, and Walter P, *Proc. Natl. Acad. Sci. USA*, **102**, 18773–18784 (2005).
5) Calfon M, Zeng H, Urano F, Till JH, Hubbard SR, Harding HP, Clark SG, and Ron D, *Nature*, **415**, 92–96 (2002).

6) Yoshida H, Matsui T, Yamamoto A, Okada T, and Mori K, *Cell*, **107**, 881–891 (2001).
7) Lee AH, Iwakoshi NN, and Glimcher LH, *Mol. Cell. Biol.*, **23**, 7448–7459 (2003).
8) Marciniak SJ and Ron D, *Physiol. Rev.*, **86**, 1133–1149 (2006).
9) Ozcan U, Cao Q, Yilmaz E, Lee AH, Iwakoshi NN, Ozdelen E, Tuncman G, Görgün C, Glimcher LH, and Hotamisligil GS, *Science*, **306**, 457–461 (2004).
10) Fujimoto T, Onda M, Nagai H, Nagahata T, Ogawa K, and Emi M, *Breast Cancer*, **10**, 301–306 (2003).
11) Shuda M, Kondoh N, Imazeki N, Tanaka K, Okada T, Mori K, Hada A, Arai M, Wakatsuki T, Matsubara O, Yamamoto N, and Yamamoto M, *J. Hepatol.*, **38**, 605–614 (2003).
12) Feldman DE, Chauhan V, and Koong AC, *Mol. Cancer Res.*, **3**, 597–605 (2005).
13) Romero-Ramirez L, Cao H, Nelson D, Hammond E, Lee AH, Yoshida H, Mori K, Glimcher LH, Denko NC, Giaccia AJ, Le QT, and Koong AC, *Cancer Res.*, **64**, 5943–5947 (2004).
14) Kaser A, Lee AH, Franke A, Glickman JN, Zeissig S, Tilg H, Nieuwenhuis EE, Higgins DE, Schreiber S, Glimcher LH, and Blumberg RS, *Cell*, **134**, 743–756 (2008).
15) Tashiro E, Hironiwa N, Kitagawa M, Futamura Y, Suzuki S, Nishio M, and Imoto M, *J. Antibiot.* (Tokyo), **60**, 547–553 (2007).
16) Futamura Y, Tashiro E, Hironiwa N, Kohno J, Nishio M, Shindo K, and Imoto M, *J. Antibiot.* (Tokyo), **60**, 582–585 (2007).
17) Kawamura T, Tashiro E, Yamamoto K, Shindo K, and Imoto M, *J. Antibiot.* (Tokyo), **61**, 303–311 (2008).
18) Kawamura T, Tashiro E, Shindo K, and Imoto M, *J. Antibiot.* (Tokyo), **61**, 312–317 (2008).
19) Elouil H, Bensellam M, Guiot Y, Vander Mierde D, Pascal SM, Schuit FC, and Jonas JC, *Diabetologia*, **50**, 1442–1452 (2007).
20) Croons V, Martinet W, Herman AG, and De Meyer GR, *J. Pharmacol. Exp. Ther.*, **325**, 824–832 (2008).
21) Sugita M, Natori Y, Sueda N, Furihata K, Seto H, and Otake N, *J. Antibiot.* (Tokyo), **35**, 1474–1479 (1982).
22) Kim WG, Song NK, and Yoo ID, *J. Antibiot.* (Tokyo), **55**, 204–207 (2002).
23) Feuerbach D, Waelchli R, Fehr T, and Feyen JH, *J. Biol. Chem.*, **270**, 25949–25955 (1995).
24) Azzam ME and Algranati ID, *Proc. Natl. Acad. Sci. USA*, **70**, 3866–3869 (1973).
25) Pestka S, *Annu. Rev. Microbiol.*, **25**, 487–562 (1971).

Bioorganic & Medicinal Chemistry Letters 21 (2011) 1385–1389

Contents lists available at ScienceDirect

Bioorganic & Medicinal Chemistry Letters

journal homepage: www.elsevier.com/locate/bmcl

Synthesis and anti-migrative evaluation of moverastin derivatives

Masato Sawada [a,†], Shin-ichiro Kubo [b,†], Koji Matsumura [b], Yasushi Takemoto [a], Hiroki Kobayashi [a], Etsu Tashiro [a], Takeshi Kitahara [b], Hidenori Watanabe [b,*], Masaya Imoto [a,*]

[a] Department of Biosciences and Informatics, Faculty of Science and Technology, Keio University, 3-14-1 Hiyoshi, Kohoku-ku, Yokohama 223-8522, Japan
[b] Graduate School of Agricultural and Life Sciences, The University of Tokyo, 1-1-1 Yayoi, Bunkyo-ku, Tokyo 113-8657, Japan

ARTICLE INFO

Article history:
Received 6 December 2010
Revised 6 January 2011
Accepted 7 January 2011
Available online 11 January 2011

Keywords:
Cell migration
Chemical synthesis
UTKO1

ABSTRACT

Cell migration of tumor cells is essential for invasion of the extracellular matrix and for cell dissemination. Inhibition of the cell migration involved in the invasion process represents a potential therapeutic approach to the treatment of tumor metastasis; therefore, a novel series of derivatives of moverastins (moverastins A and B), an inhibitor of tumor cell migration, was designed and chemically synthesized. Among these moverastin derivatives, several compounds showed stronger cell migration inhibitory activity than parental moverastins, and UTKO1 was found to have the most potent inhibitory activity against the migration of human esophageal tumor EC17 cells in a chemotaxis cell chamber assay. Interestingly, although moverastins are considered to inhibit tumor cell migration by inhibiting farnesyltransferase (FTase), UTKO1 did not inhibit FTase, indicating that UTKO1 inhibited tumor cell migration by a mechanism other than the inhibition of FTase.

Despite significant advances in understanding the fundamental aspects of cancer, the development of metastatic lesions remains the predominant cause of death for most cancer patients.[1,2] Cell migration is a crucial event in the spread of cancer and, consequently, the metastatic process.[3,4] This prompted us to develop inhibitors of tumor cell migration as novel anti-metastatic drugs.

Previously, we screened for inhibitors of cancer cell migration derived from microbial origin, and obtained moverastin A and B (**1** and **2**, respectively), new members of the cylindrol family, from *Aspergillus* sp. F7720.[5] Their structures including the absolute stereochemistries were confirmed unambiguously by the synthesis as outlined in Scheme 1. Furthermore, moverastin A and B were found to inhibit FTase; therefore, moverastins were considered to inhibit the migration of tumor cells by inhibiting the farnesylation of H-Ras, and subsequent H-Ras-dependent activation of the PI3K/Akt pathway. However, because the inhibitory activity of moverastins for tumor cell migration was rather modest (IC_{50} value of 7 μM), we considered it an attractive lead compound in the search for other, more potent agents.

In this study, we chemically synthesized a series of moverastin derivatives and assessed their potential as tumor cell migration inhibitors in several in vitro assays.

Structures of moverastin derivatives (UTKO1–12) synthesized in this study are shown in Figure 1. UTKO1–6 were synthesized by employing the same approach as that for our previous synthesis of moverastins.[5] The enol triflates (**7**, **10**, **12**, **15**, **18**) were prepared starting from readily available ketones or aldehydes (**5**, **9**, **11**, **13**, **16**, respectively) as shown in Scheme 2. Coupling reactions between the enol triflates (or 2-iodopropene for UTKO4) and aldehyde **4** were carried out successfully using the Nozaki–Hiyama–Kishi procedure[6,7] and UTKO1–6 were obtained after acid hydrolysis of MOM ether. The dihydro analog (UTKO7) and etherified analogs (UTKO9 and 10) of UTKO1 were also synthesized by its hydrogenation, Mitsunobu reaction or methylation (Scheme 3). The unsaturated ketone analog of UTKO1 was also obtained by the PDC oxidation-deprotection of **19** which is the intermediate from **7** to UTKO1. UTKO11 and 12, deformylated analogs of moverastin and UTKO1, respectively, were also synthesized from aldehyde **21** instead of **4** (Scheme 4). Detailed synthetic procedure for UTKO compounds will be published elsewhere.

Next, the cell migration inhibitory activity of these moverastin derivatives was examined by the chemotaxis cell chamber (BD Biosciences) assay using conditioned medium of human esophageal tumor EC17 cells as a source of chemoattractants as previously reported with some modifications.[8] In this assay, EC17-conditioned medium was initially placed in the lower compartment. EC17 cells were incubated in the upper chamber, where they were allowed to migrate and penetrate the filter separating the chambers in order to enter the lower chamber. After 24 h of incubation, the number of cells attached to the lower side of the filter was counted. The IC_{50} values obtained in this study are listed in Table 1. Among

* Corresponding authors. Tel./fax: +81 45 566 1557 (M.I.); tel.: +81 3 5841 5119; fax: +81 3 5841 8019 (H.W.).
E-mail addresses: ashuten@mail.ecc.u-tokyo.ac.jp (H. Watanabe), imoto@bio.keio.ac.jp (M. Imoto).
† These authors contributed equally to the study.

0960-894X/$ - see front matter © 2011 Elsevier Ltd. All rights reserved.
doi:10.1016/j.bmcl.2011.01.028

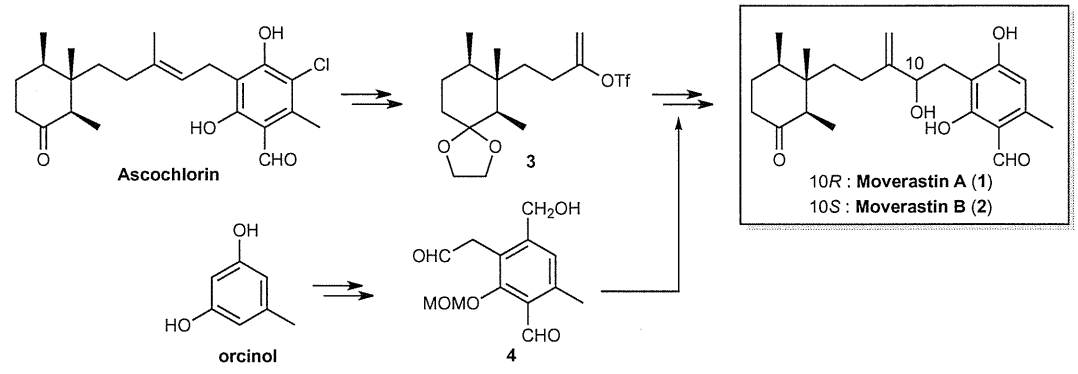

Scheme 1. Synthesis and structures of moverastin A and B.

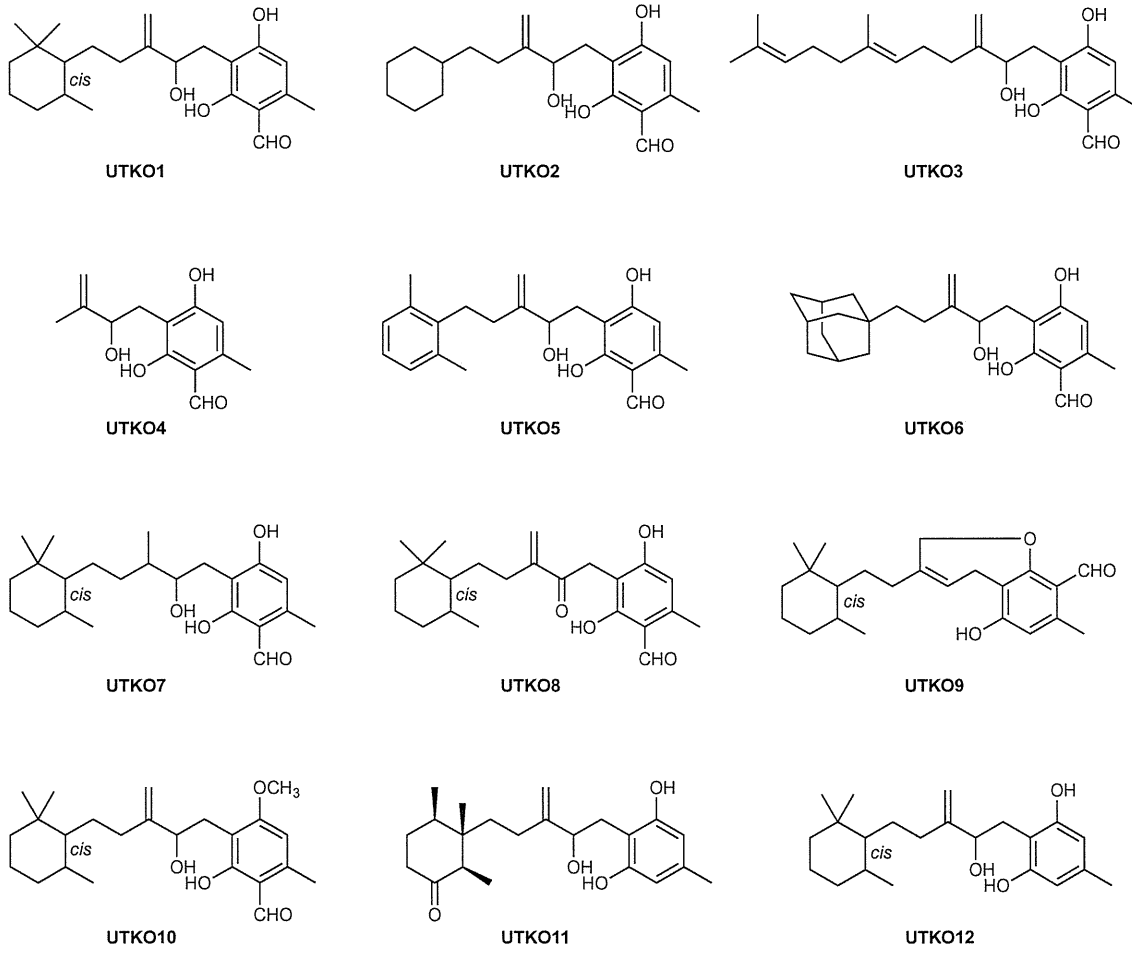

Figure 1. Structures of moverastin derivatives.

moverastin derivatives, UTKO1 showed the most potent inhibitory activity of EC17 cell migration with an IC_{50} of 1.98 μM (Fig. 2). UTKO7, UTKO9 and UTKO12 are also significantly more active inhibitors of EC17 cell migration than the parental natural product, moverastin A, with IC_{50} values of 2.12, 2.00 and 2.17 μM, respectively (Table 1). These inhibitory effects are not due to the toxic effect of the drug because their 50% inhibitory concentration for EC17 cell viability, as estimated by trypan blue dye exclusion assay, was at least five-fold higher than that for cell migration.

Previously, we found that moverastin A showed inhibitory activity against FTase, and demonstrated that moverastin A inhibited the migration of tumor cells by inhibiting the farnesylation of H-Ras;[5] therefore, next we examined the effect of moverastin derivatives on FTase in vitro. For this assay, FTase was partially purified from EC17 cells and recombinant GST-H-Ras and [^{3}H]-farnesylpyrophosphate were used as the substrates as described before.[5] As shown in Table 1, all moverastin derivatives tested, including UTKO1, UTKO7, UTKO9, and UTKO12, which showed strong inhibition of cell migration, did not inhibit FTase in vitro up to 100 μM. These results indicated that a mechanism other than the inhibition of FTase is responsible for UTKO-induced inhibition of EC17 cell migration. To examine this possibility, several cancer

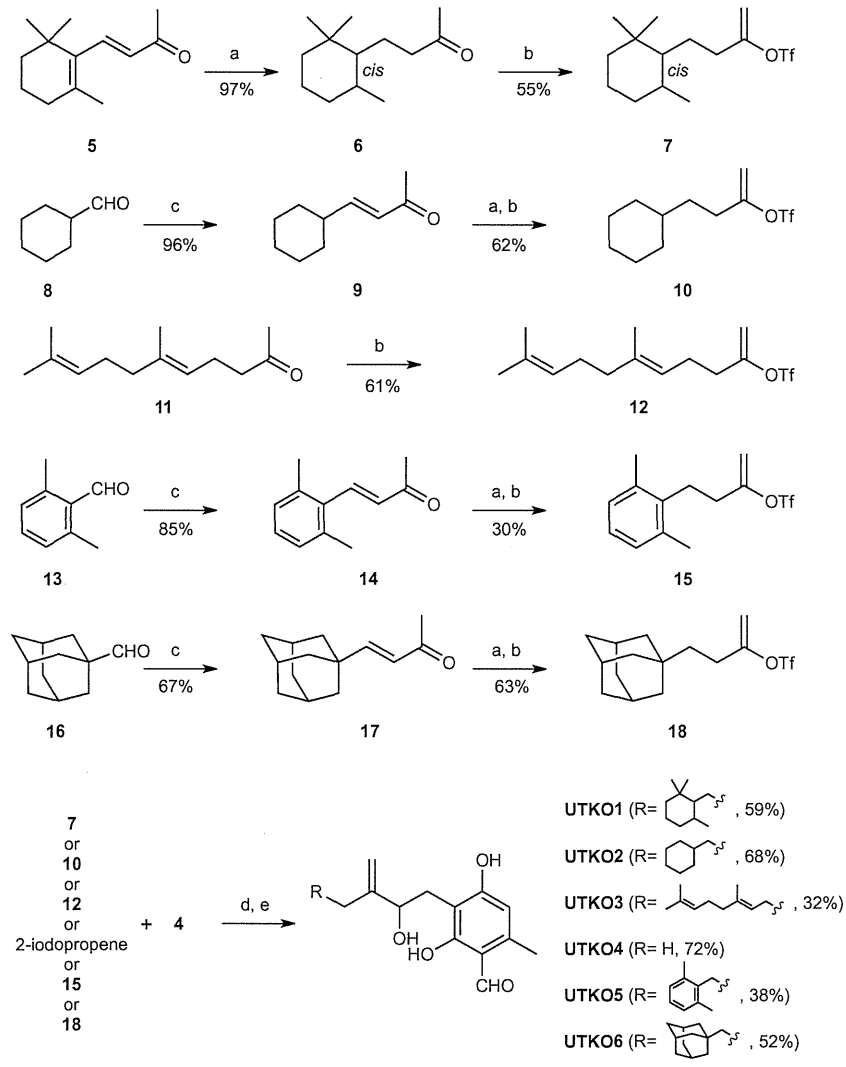

Scheme 2. Synthesis of UTKO1–6. Reagents and conditions: (a) H_2, Pd-C, EtOAc (for **6**) or EtOH (for **10**, **15** and **18**); (b) KHMDS, Comin's reagent, THF, −78 °C; (c) $Ph_3P{=}CHCOMe$, CH_2Cl_2 (for **9** and **14**) or xylene (for **17**), reflux; (d) $CrCl_2$, $NiCl_2$, DMF, rt; (e) concd HCl, THF, rt.

cell lines were investigated with respect to the inhibitory potential of moverastin A and the most potent moverastin derivative, UTKO1. The inhibitory effect of moverastin A depends on cell type, and there is a significant negative correlation between the sensitivity of each cell to moverastin A and the expression level of H-Ras, a substrate of FTase ($r = -0.86$, $p = 0.0013$) (Fig. 3). This result

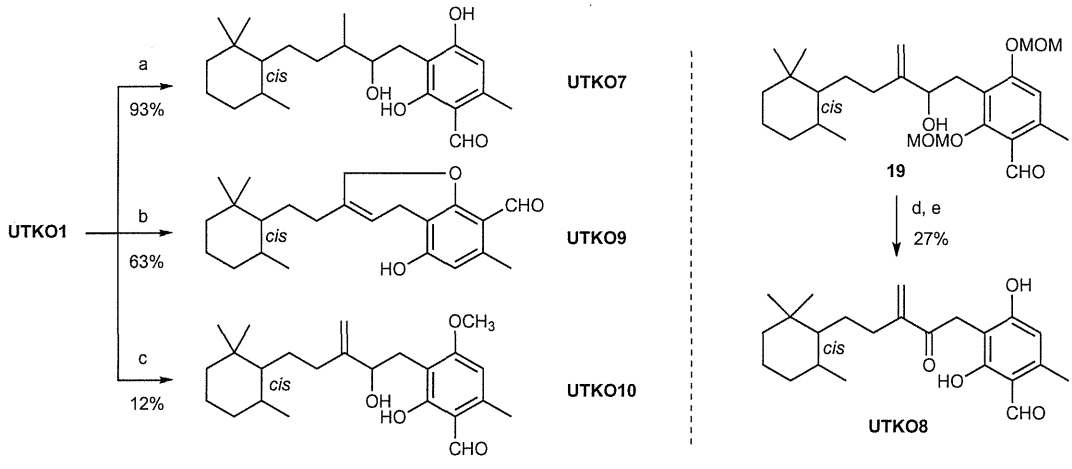

Scheme 3. Synthesis of UTKO7–10. Reagents and conditions: (a) Rh-Al_2O_3, EtOH; (b) DEAD, PPh_3, THF; (c) MeI, K_2CO_3, $(n\text{-}Bu)_4N{\cdot}HSO_4$, EtOAc–toluene, reflux; (d) PDC, CH_2Cl_2; (e) concd HCl, THF, rt.

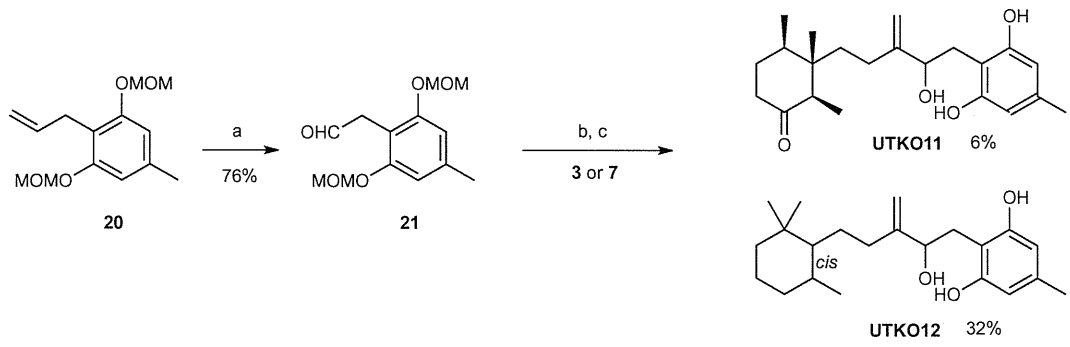

Scheme 4. Synthesis of UTKO11 and UTKO12. (a) O_3, CH_2Cl_2, −78%, then PPh_3; (b) $CrCl_2$, $NiCl_2$, DMF, rt; (c) concd HCl, THF, rt.

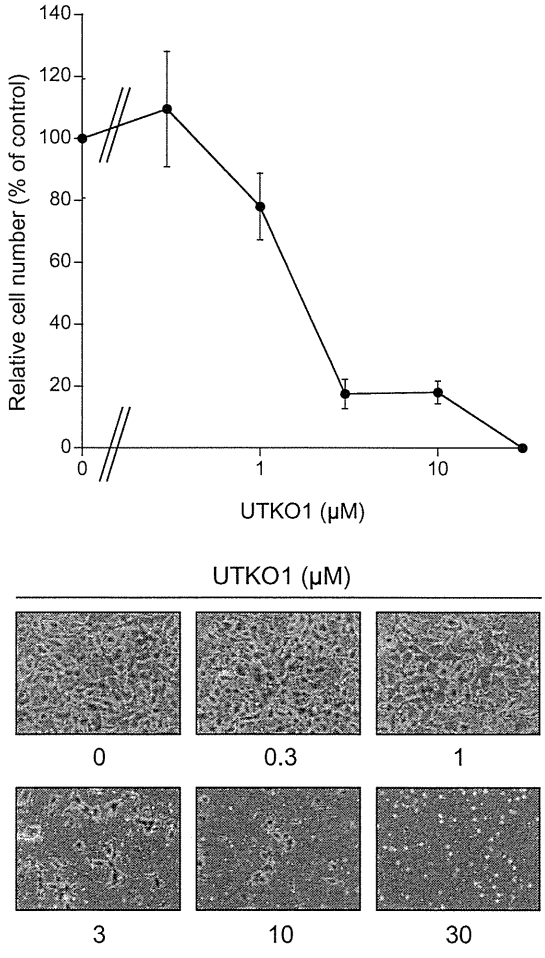

Figure 2. Effect of UTKO1 on migration of EC17 cells. EC17 cells were incubated with various concentrations of UTKO1 in the top chamber; the lower chamber contained EC17-conditioned medium, obtained from 24-hour cultures of EC17 cells maintained in RPMI1640 supplemented with 1% FBS. After 24 h, the number of cells that migrated through the filter to the lower surface was counted. The results are the mean ± SD of five different fields.

supported our previous conclusion that moverastins inhibited tumor cell migration due to the inhibition of FTase. On the other hand, the cell migration inhibitory activity of UTKO1 also depends on cell type, but there is no correlation with the expression levels of H-Ras ($r = -0.38$, $p = 0.40$) (Fig. 3). These results suggested that the inhibitory mechanism of cell migration by UTKO1 is different from that of moverastin A. To understand the molecular basis by which UTKO1 inhibits tumor cell migration, biochemical identification of the protein target for UTKO1 is now under investigation.

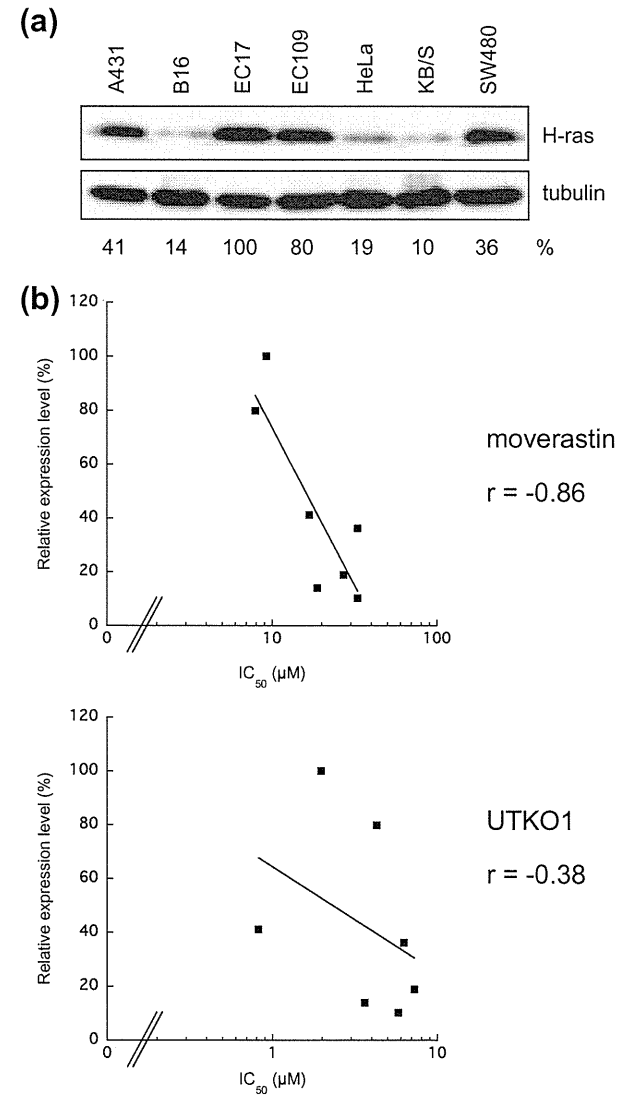

Figure 3. Correlation between expression levels of H-Ras and inhibition of migration by moverastin A and UTKO1. (a) Western blot analysis of H-Ras expression levels in seven tumor cell lines. Cell lysates were separated by SDS-PAGE and then subjected to immunoblotting using anti-H-Ras antibody. Quantitation of expression levels of H-Ras was analyzed by Image gauge and normalized with the level of tubulin. Percentages represent the relative expression level of H-Ras in tumor cells compared to the level in EC17 cells. (b) Simple linear correlations between two parameters were calculated. Correlation coefficients (r) are shown in this figure.

Table 1
Effects of UTKO compounds on cell migration, cell viability and in vitro FTase activity in EC17 cells

	IC_{50} (μM)		
	Cell migration	Cell viability[a]	FTase[b]
Moverastin A	7.22	>77	14.7
UTKO1	1.98	46	>100
UTKO2	8.43	87	>100
UTKO3	7.53	>80	>100
UTKO4	30.0	>130	>100
UTKO5	10.6	45	>100
UTKO6	6.52	55	>100
UTKO7	2.12	16	>100
UTKO8	4.41	18	>100
UTKO9	2.00	18	>100
UTKO10	4.57	18	>100
UTKO11	21.4	>28	>100
UTKO12	2.17	17	>100

[a] For cell viability assay, a trypan blue dye (15250-061, Gibco, Invitrogen) exclusion assay were used to examine cell viability and performed according to previously reported protocols.[9]

[b] For in vitro FTase assay, partially purified enzymes from EC17 cells were incubated with [^{3}H]-FPP plus recombinant GST-H-Ras in the presence or absence of test compound. The reaction was terminated by the addition of TCA. The radioactivity of the TCA insoluble fraction was measured.

Our preliminary structure–activity relationship study revealed that UTKO12 retained the same level of inhibitory activity toward EC17 cell migration as that of UTKO1, indicating that formyl group on benzene ring is not required for the inhibitory activity toward EC17 cell migration. On the other hand, the formyl groups of moverastins are essential for the FTase inhibition, because the inhibitory activity of UTKO11 toward FTase has been lost.

Although UTKO1 was initially synthesized as an analogous compound of moverastins, it possesses a different biological function from cylindrol family, and therefore, UTKO1 is expected to be a new lead compound in the search for more potent anti-metastatic and anti-cancer agents.

Acknowledgement

This work was supported by a grant from the Ministry of Education, Culture, Sports, Science, and Technology.

Supplementary data

Supplementary data associated with this article can be found, in the online version, at doi:10.1016/j.bmcl.2011.01.028. These data include MOL files and InChiKeys of the most important compounds described in this article.

References and notes

1. Gupta, P. B.; Mani, S.; Yang, J.; Hartwell, K.; Weinberg, R. A. *Cold Spring Harb. Symp. Quant. Biol.* **2005**, *70*, 291.
2. Gupta, G. P.; Massague, J. *Cell* **2006**, *127*, 679.
3. Chambers, A.; Groom, A.; MacDonald, I. *Nat. Rev. Cancer* **2002**, *2*, 563.
4. Friedl, P.; Wolf, K. *Nat. Rev. Cancer* **2003**, *3*, 362.
5. Takemoto, Y.; Watanabe, H.; Uchida, K.; Matsumura, K.; Nakae, K.; Tashiro, E.; Shindo, K.; Kitahara, T.; Imoto, M. *Chem. Biol.* **2005**, *12*, 1337.
6. Takai, K.; Kimura, K.; Kuroda, T.; Hiyama, T.; Nozaki, H. *Tetrahedron Lett.* **1983**, *24*, 5281.
7. Takai, K.; Tagashira, M.; Kuroda, T.; Oshima, K.; Utimoto, K.; Nozaki, H. *J. Am. Chem. Soc.* **1986**, *108*, 6048.
8. Saiki, I.; Murata, J.; Yoneda, J.; Kobayashi, H.; Azuma, I. *Int. J. Cancer* **1994**, *56*, 867.
9. Ormerod, M. G.; Collins, M. K.; Rodriguez-Tarduchy, G.; Robertson, D. *J. Immunol. Methods* **1992**, *153*, 57.

ORGANIC LETTERS
2010
Vol. 12, No. 21
5068–5071

Total Synthesis of Incednam, the Aglycon of Incednine

Takashi Ohtani,[†] Shinya Tsukamoto,[†] Hiroshi Kanda,[†] Kensuke Misawa,[†] Yoshifumi Urakawa,[†] Takahiro Fujimaki,[‡] Masaya Imoto,[‡] Yoshikazu Takahashi,[§] Daisuke Takahashi,[†] and Kazunobu Toshima*[,†]

Department of Applied Chemistry and Department of Biosciences and Informatics, Faculty of Science and Technology, Keio University, 3-14-1 Hiyoshi, Kohoku-ku, Yokohama 223-8522, Japan, and Institute of Microbial Chemistry, 3-14-23 Kamiosaki, Shinagawa-ku, Tokyo 141-0021, Japan

toshima@applc.keio.ac.jp

Received October 5, 2010

ABSTRACT

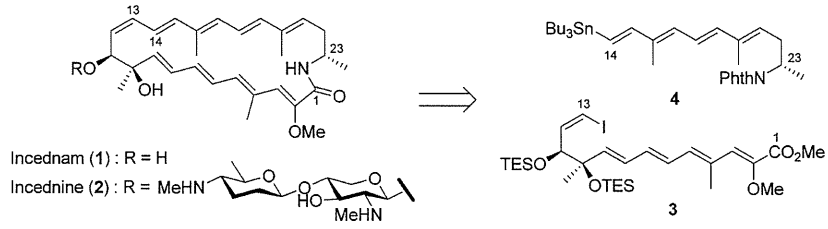

The first total synthesis of incednam (1), the aglycon of antibiotic incednine (2), is described. Incednine has been reported to exhibit significant inhibitory activity against the antiapoptotic oncoproteins Bcl-2 and Bcl-xL. The synthesis of 1 commenced with the preparation of the C1–C13 subunit 3 and the C14–C23 subunit 4. The construction of the novel 24-membered macrocycle was achieved by the application of a Stille coupling between 3 and 4, followed by macrolactamization.

Incednam (**1**) is the aglycon of the 24-membered macrolactam glycoside antibiotic incednine (**2**), which was isolated from *Streptomyses* sp. in 2008.[1] It was demonstrated that **2** exhibits significant inhibitory activity against the antiapoptotic oncoproteins Bcl-2 and Bcl-xL, with a mode of action distinctly different from those of other compounds that inhibit the binding capacity of Bcl-xL to the pro-apoptotic protein Bax. In addition, it is known that these proteins are overexpressed in many cancer cells, resulting in the expansion of a transformed population and the advancement of the multidrug-resistant stage.[2–4] Therefore, **2** is now expected to be a compound in the development of novel antitumor drugs. Furthermore, **2** is likely to be a useful tool for the further study of Bcl-2 and Bcl-xL functions. The identification of its target protein could provide insight into the antiapoptotic mechanism of the Bcl-2 family proteins. From a structural perspective, **1** and **2** contain unique salient features: an α-methoxy-α,β-unsaturated amide moiety and two independent conjugated polyene systems embedded in the 24-membered macrolactam ring. As a result of the nature of the highly conjugated polyene subunits, **1** and **2** are light- and acid-sensitive. Although **1** was also isolated from *Streptomyses* sp.,[1] its semisynthesis from **2** has not been realized, in part, because of the inherent chemical instabilities mentioned above. Furthermore, the stereochemical configuration at C23 was postulated on the basis of computational modeling studies, thus the configuration has not been conclusively defined. Because of its important biological

[†] Department of Applied Chemistry.
[‡] Department of Biosciences and Informatics.
[§] Institute of Microbial Chemistry.

(1) Futamura, Y.; Sawa, R.; Umezawa, Y.; Igarashi, M.; Nakamura, H.; Hasagawa, K.; Yamasaki, M.; Tashiro, E.; Takahashi, Y.; Akamatsu, Y.; Imoto, M. *J. Am. Chem. Soc.* **2008**, *130*, 1822.
(2) Tsujimoto, Y.; Finger, L. R.; Yunis, J.; Nowell, P. C.; Croce, C. M. *Science* **1984**, *226*, 1097.
(3) Reed, J. C.; Cuddy, M.; Slabiak, T.; Croce, C. M.; Nowell, P. C. *Nature* **1988**, *336*, 259.
(4) Gross, A.; McDonnell, J. M.; Korsmeyer, S. J. *Gene Dev.* **1999**, *13*, 1899.

10.1021/ol102400c
Published on Web 10/12/2010

activity and novel molecular architecture, **1** and **2** were considered to be prime targets for chemical synthesis. Herein we report the first total synthesis of **1** leading to the unambiguous stereochemical assignment of the configuration at C23.

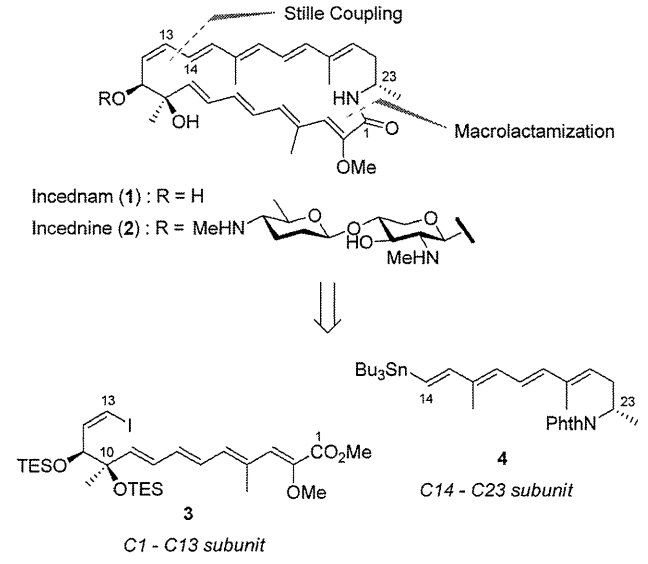

Figure 1. Retrosynthetic analysis of incednam (**1**).

The retrosynthetic analysis of **1** is depicted in Figure 1. The convergent strategy implemented toward the construction of the novel 24-membered macrocycle is based on the coupling of two domains: the C1−C13 subunit **3** containing the vinyl iodide moiety and the C14−C23 subunit **4** containing the vinyl stannane moiety. This union could be effected by the application of a Stille coupling and subsequent macrolactamization. Our group recently reported an asymmetric synthesis of **3**,[5] employing a Sharpless asymmetric epoxidation as the key step. However, in this sequence an optical resolution involving the stoichiometric use of an optical resolution agent was required to provide the enantiomerically pure subunit **3**. To circumvent this issue, we first developed a direct synthetic route toward the stereochemically pure subunit **3**, which was facilitated by an Evans aldol addition thereby establishing the C10 and C11 stereocenters.

The synthesis of the pentaenoate subunit **3**, corresponding to C1−C13 in **1**, is summarized in Scheme 1. The known 1,3-diol **9**[6] was prepared from methyl L-lactate (**5**). Benzylation of **5** and subsequent coupling with the chiral auxiliary **6**[7] provided the oxazolidinone derivative **7**. Following Kobayashi's procedure, the titanium-mediated Evans aldol addition of **7** with *trans*-crotonaldehyde using $Ti(O^iPr)_3Cl$

Scheme 1. Synthesis of the C1−C13 Subunit **3**

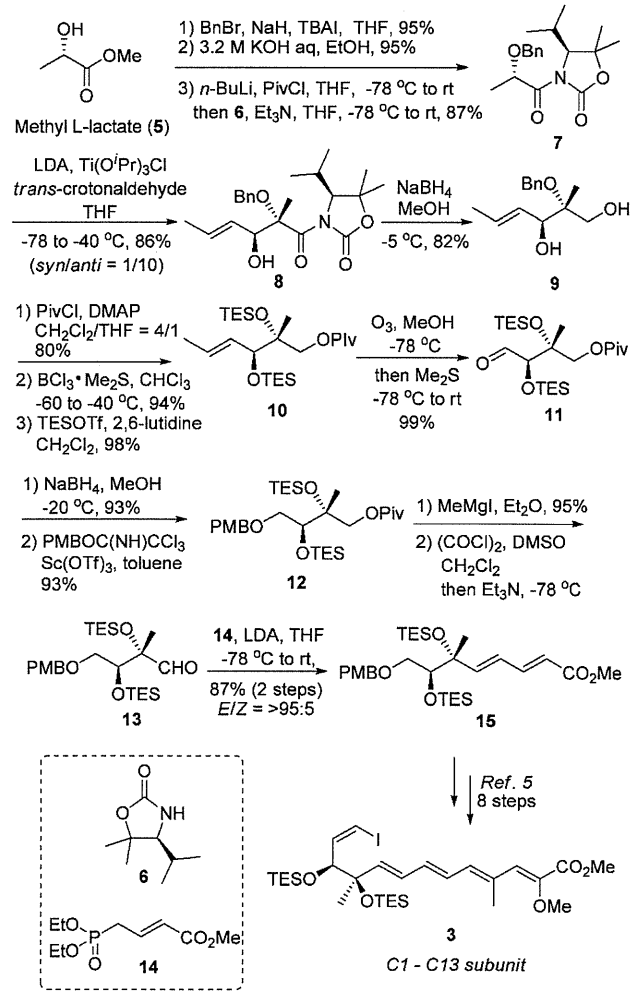

and LDA proceeded smoothly to give the desired Evans *anti* product **8** in 86% yield with high diastereoselectivity (dr =10:1). Subsequent cleavage of the chiral auxiliary in **8** with $NaBH_4$ provided the diol **9** in 82% yield. The primary alcohol was selectively protected as the pivaloyl ester, and the benzyl ether was cleaved using $BCl_3{\cdot}Me_2S$[8] without affecting the pendant olefin. The resulting diol was subsequently protected using TESOTf and 2,6-lutidine to give the silyl ether **10** (74% overall yield). The disubstituted olefin was oxidatively cleaved with ozone to afford the aldehyde **11**, which was reduced with $NaBH_4$ to provide the primary alcohol. Protection of the resulting primary alcohol as the PMB ether using PMB trichloroacetimidate and $Sc(OTf)_3$,[9] provided **12** (86% overall yield from **10**). Cleavage of the pivaloyl ester in **12** using MeMgI,[10] without migration of the silyl groups, followed by Swern oxidation gave the aldehyde **13**. Horner−Wadsworth−Emmons olefination of **13** with the phosphonate ester **14**[11] provided the $\alpha,\beta,\gamma,\delta$-unsaturated ester

(5) Ohtani, T.; Kanda, H.; Misawa, K.; Urakawa, Y.; Toshima, K. *Tetrahedron Lett.* **2009**, *50*, 2270.
(6) Murata, Y.; Kamino, T.; Hosokawa, S.; Kobayashi, S. *Tetrahedron Lett.* **2002**, *43*, 8121.
(7) Evans, D. A.; Bartroli, J.; Shih, T. L. *J. Am. Chem. Soc.* **1981**, *103*, 2127.
(8) Qureshi, S.; Shaw, G. *J. Chem. Soc., Perkin Trans. 1* **1985**, 875.
(9) Trost, B. M.; Waser, J.; Meyer, A. *J. Am. Chem. Soc.* **2008**, *130*, 16424.
(10) Heys, R. *J. Chem. Soc., Chem. Commun.* **1992**, 680.
(11) Barth, R.; Mulzer, J. *Tetrahedron* **2008**, *64*, 4718.

15 in high yield with high stereoselectivity (83% overall yield from **12** with E:Z = >95:5). The building block **15** was an intermediate in our previous studies and was converted into the C1−C13 subunit **3** in 8 steps in high overall yield.[5]

Next, the synthesis of the C14−C23 subunit **4** was established starting from the commercially available alcohol **16** as shown in Scheme 2. The one-pot Swern oxidation−Wittig olefination[12]

Scheme 2. Synthesis of the C14−C23 Subunit **4**

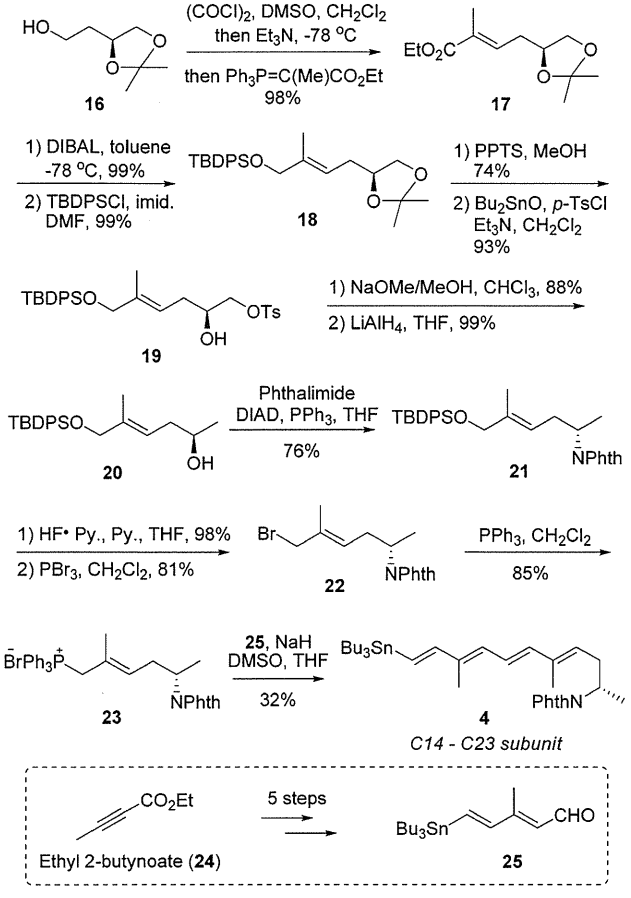

of **16** gave the α,β-unsaturated ester **17** in 98% yield with complete stereoselectivity. After the reduction of **17** with DIBAL, the resulting allylic alcohol was protected as the TBDPS ether in 98% overall yield. Deprotection of the acetonide in **17** under acidic conditions and subsequent selective tosylation of the resulting primary alcohol using Bu_2SnO, p-TsCl and Et_3N[13] afforded **19**. The intramolecular epoxide formation using NaOMe, followed by the selective ring opening of the resulting epoxide with $LiAlH_4$, led to **20** (60% overall yield from **18**). The secondary alcohol **20** was converted into the N-substituted phthalimide **21** with stereochemical inversion by the Mitsunobu reaction using phthalimide, DIAD, and PPh_3 in 76% yield. Deprotection of the TBDPS ether in **21** with HF•pyridine and subsequent bromination with PBr_3 provided the allylic bromide **22** without olefin isomerization; **22** was readily converted into the phosphonium salt **23** (67% overall yield from **21**). The Wittig olefination of **23** with the known aldehyde **25**[14] (prepared from ethyl 2-butynoate (**24**) in 5 steps) was examined under several conditions. As a result, it was found that the desired E-configured tetraene **4** could be obtained in 32% yield by using NaH and DMSO in THF[15] at 0 °C. Because **4** is extremely prone to oxidation and/or photochemical decomposition, it was used in the next step immediately after isolation. Considering the inherent convergency of the chemical union of **23** and **25**, the modest yield obtained in the olefination reaction is well justified. This strategy leads to the direct construction of the labile tetraene **4**, which contains the vinyl stannane moiety necessary for the subsequent Stille coupling.

Completion of the synthesis of **1** is summarized in Scheme 3. Conditions for the Stille coupling[16] of **3** with **4** was

Scheme 3. Total Synthesis of Incednam (**1**)

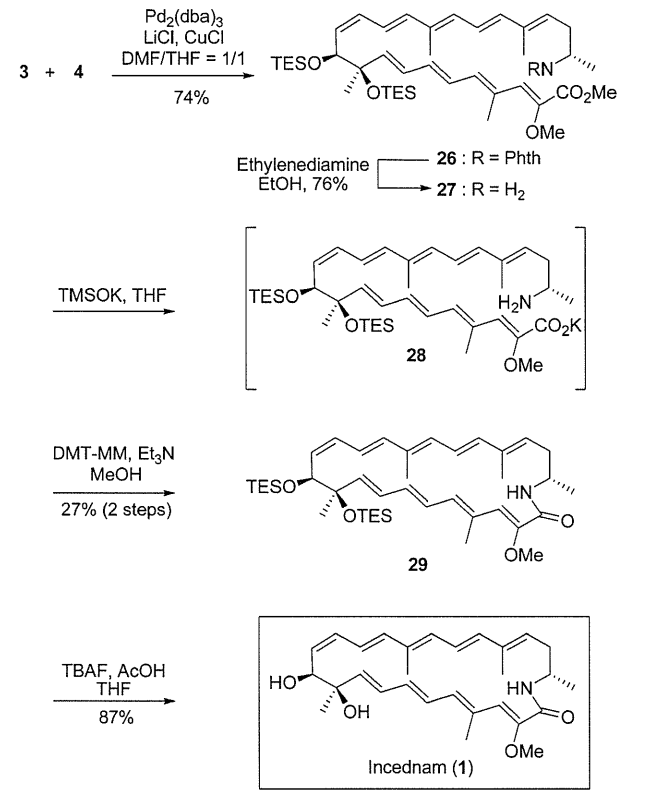

rigorously explored. After much experimentation, it was found that Corey's protocol[17] using Pd(0), LiCl, and CuCl gave the best result, providing the desired coupling product **26** in 74% yield. Removal of the phthaloyl group in **26** using ethylenediamine provided the amine **27** in 76%

(12) Labelle, M.; Morton, H. E.; Guindon, Y.; Springer, J. P. *J. Am. Chem. Soc.* **1988**, *110*, 4533.

(13) Michael, J. M.; Naresh, K. N.; Eric, D. M.; Ulhas, P. D.; Joseph, M. P.; Rajappa, M. *Org. Lett.* **1999**, *1*, 447.

(14) (a) Betzer, J. F.; Delaloge, F.; Muller, B.; Panqrazi, A.; Pruner, J. *J. Org. Chem.* **1997**, *62*, 7768. (b) Michels, D. T.; Uhee, J. U.; Vanderwal, C. D. *Org. Lett.* **2008**, *10*, 4787.

(15) Tatsuta, K.; Nakagawa, A.; Maniwa, S.; Kinoshita, M. *Tetrahedron Lett.* **1980**, *21*, 1479.

(16) Milstein, D.; Stille, J. K. *J. Am. Chem. Soc.* **1979**, *101*, 4992.

(17) Han, X.; Stoltz, B. M.; Corey, E. J. *J. Am. Chem. Soc.* **1999**, *121*, 7600.

yield. Saponification of the methyl ester in **27** using TMSOK,[18] followed by treatment using reversed phase column chromatography, provided the potassium carboxylate **28**. Without further purification, macrolactamization of **28** utilizing DMT-MM[19] in MeOH was conducted. Gratifyingly, it was found that the macrolactamization proceeded smoothly to give the desired cyclic compound **29** in 27% overall yield from **27**. Deprotection of the TES groups in **29** was effected with TBAF and AcOH to furnish incednam (**1**). Data for an analytical sample of the synthetic incednam obtained by ^{1}H NMR, ^{13}C NMR, HRMS (ESI-TOF), and optical rotation matched those obtained for an authentic sample.[1] These results clearly confirm not only the complete synthesis of **1**, but also serve to conclusively establish the stereochemical configuration at C23 (*S* configuration), which was previously posited purely on the basis of molecular modeling.

(18) Laganis, E. D.; Chenard, B. L. *Tetrahedron Lett.* **1984**, *25*, 5831.
(19) Kunishima, M.; Kawachi, C.; Hioki, K.; Terao, K.; Tani, S. *Tetrahedron* **2001**, *57*, 1551.

In conclusion, we have developed a convergent synthetic route to incednam (**1**), which is the aglycon of the 24-membered macrolactam glycoside antibiotic incednine (**2**). Furthermore, this synthesis serves to unambiguously define the stereochemical configuration at C23 in **1**. Additional studies with respect to the total synthesis of incednine (**2**) from **1** are currently underway in our laboratory.

Acknowledgment. With great respect, we dedicate this work to Professor Kuniaki Tatsuta on the occasion of his 70th birthday. This research was supported in part by the 21st Century COE Program "Keio Life-Conjugated Chemistry", High-Tech Research Center Project for Private Universities: Matching Fund Subsidy, 2006-2011, and JSPS Fellow 22•5820 from the Ministry of Education, Culture, Sports, Science and Technology of Japan (MEXT).

Supporting Information Available: Experimental procedures and compound characterizations. This material is available free of charge via the Internet at http://pubs.acs.org.

OL102400C

Chemistry & Biology
Article

Metabolomic Identification of the Target of the Filopodia Protrusion Inhibitor Glucopiericidin A

Mitsuhiro Kitagawa,[1,3] Satsuki Ikeda,[2] Etsu Tashiro,[1] Tomoyoshi Soga,[2] and Masaya Imoto[1,*]
[1]Department of Biosciences and Informatics, Faculty of Science and Technology, Keio University, 3-14-1 Hiyoshi, Kohokuku, Yokohama, Kanagawa 223-8522, Japan
[2]Institute for Advanced Biosciences, Keio University, 246-2, Mizukami, Kakuganji, Tsuruoka, Yamagata 997-0052, Japan
[3]Present address: Institute for Advanced Biosciences, Keio University, 246-2, Mizukami, Kakuganji, Tsuruoka, Yamagata, 997-0052, Japan
*Correspondence: imoto@bio.keio.ac.jp
DOI 10.1016/j.chembiol.2010.06.017

SUMMARY

Identifying the targets of bioactive compounds is a major challenge in chemical biological research. Here, we identified the functional target of the natural bioactive compound glucopiericidin A (GPA) through metabolomic analysis. We isolated GPA while screening microbial samples for a filopodia protrusion inhibitor. Interestingly, GPA alone did not inhibit filopodia protrusion, but synergistically inhibit protrusion with the mitochondrial respiration inhibitor, piericidin A (PA). These results suggested that GPA might inhibit glycolysis. Capillary electrophoresis time-of-flight mass spectrometry (CE-TOFMS) provided strong evidence that GPA suppresses glycolysis by functionally targeting the glucose transporter. GPA may therefore serve as a glucose transporter chemical probe. Simultaneous inhibition of both glycolysis and mitochondrial respiration dramatically decreased intracellular ATP levels, indicating that GPA inhibits ATP-dependent filopodia protrusion with PA. Our results represent a challenge of molecular target identification using metabolomic analysis.

INTRODUCTION

To fully understand the regulation of cellular events (e.g., cell growth, survival, migration), functional analysis of each protein involved in the regulatory systems is required (Pandey and Mann, 2000). Genetic studies utilizing chemical inhibitors are among the best approaches to investigate protein function (Alaimo et al., 2001; Zheng and Chan, 2002). Chemical inhibitors can be used to modulate the function of target proteins in a manner analogous to the engineering of mutations in molecular genetic studies (Alaimo et al., 2001; Fenteany et al., 1995; Liu et al., 1991). Many chemical inhibitors are available, though there are far fewer than the number of proteins involved in the complicated regulation of cellular events. Therefore, new chemical inhibitors must be developed in order to advance the applicability of chemical genetic studies to the functional analysis of proteins.

The structural diversity of natural products makes them ideal screening sources for chemical inhibitors that can be used to dissect the complex molecular mechanisms underlying cellular events through chemical genetics (Abel et al., 2002; Newman and Cragg, 2007). One strategy for screening natural products for new chemical inhibitors is the cell-based assay (Hart, 2005). However, identifying the target of a molecular inhibitor isolated by cell-based assays represents a crucial hurdle that must be overcome before chemical genetic studies can commence.

There are two fundamental approaches to identify chemical inhibitor targets: direct and indirect (Hart, 2005). In the direct approach, the target proteins bound to the inhibitor are purified and directly identified by mass spectrometry. In this approach, chemical synthesis of the inhibitor compound onto immobilized beads or a column is required for affinity purification of the binding proteins. However, in some cases, the chiral centers and unique structural scaffolds of natural products make synthesis difficult.

The indirect approach to chemical inhibitor target identification involves searching for candidates by profiling biological data. If the compound was found to perturb some cellular event for which the regulatory signaling pathway is known, targets can be revealed by examining the effect of the compound on each step of the pathway. In some cases, omics studies (e.g., proteomics, transcriptomics, metabolomics) can aid the comprehensive investigation of a compound's effect on the potentially large numbers of biological steps (Hart, 2005).

We employed an indirect approach, using metabolomics to identify the chemical inhibitor derived from natural product screening. Metabolomics technologies have advanced tremendously in recent years, and capillary electrophoresis time-of-flight mass spectrometry (CE-TOFMS) has emerged as a powerful new tool for the comprehensive analysis of cellular metabolites (Monton and Soga, 2007; Soga et al., 2003). The use of CE-TOFMS to understand global metabolism at the system level has become widespread (Hirayama et al., 2009; Ishii et al., 2007; Soga et al., 2006; Sugimoto et al., 2009). Analysis of the metabolome with CE-TOFMS also revealed metabolic changes induced by drug compounds (Soga et al., 2006). Thus, despite a lack of reports describing the identification of chemical

Table 1. Inhibitory Activities of Remixing Silica Gel Chromatography Fractions, and the Effect of Withholding Each Fraction from the Remix

	Fractions Eluted with $CHCl_3$: MeOH						
	100: 0	100: 1	100: 2	100: 5	100: 10	100: 30	
Sample #	I	II	III	IV	V	VI	Filopodia Protrusion
Remix	Contained	Contained	Contained	Contained	Contained	Contained	Inhibition
Remix – **I**		Contained	Contained	Contained	Contained	Contained	**No inhibition**
Remix – **II**	Contained		Contained	Contained	Contained	Contained	Inhibition
Remix – **III**	Contained	Contained		Contained	Contained	Contained	Inhibition
Remix – **IV**	Contained	Contained	Contained		Contained	Contained	**No inhibition**
Remix – **V**	Contained	Contained	Contained	Contained		Contained	Inhibition
Remix – **VI**	Contained	Contained	Contained	Contained	Contained		Inhibition
I + **IV**	Contained			Contained			**Inhibition**
I	Contained						No inhibition
IV				Contained			No inhibition

See Figure S1 for the bioassay-guided isolation of the compounds.

inhibitor targets using metabolomic analysis, such efforts would be worthwhile.

We began our investigation by conducting a natural product screening to isolate bioactive compounds that inhibit cellular filopodia protrusion in the carcinoma. Filopodia are spike-like cell membrane projections contributing to tumor metastasis; however, the molecular mechanisms controlling filopodia protrusion are complicated and unclear (Faix and Rottner, 2006; Mattila and Lappalainen, 2008). Finding a filopodia inhibitor in carcinoma and its molecular target that could be employed in chemical genetic studies may therefore lead to a fuller understanding of filopodia contributing to the treatment of tumor metastasis (Bacon et al., 2007; Shulman et al., 2009). Here, we describe the isolation of a new chemical inhibitor of filopodia protrusion through natural product screening, and identification of the inhibitor's target by metabolomic analysis. This is the first report to our knowledge on natural product target molecule identification using a metabolomic approach.

RESULTS

Screening and Isolation of the Inhibitor of Filopodia Protrusion

Human epidermal carcinoma A431 cells highly express the epidermal growth factor (EGF) receptor. In response to EGF stimulation, these cells become highly chemotactic (Rabinovitz et al., 1999). Within 30 min of EGF stimulation, A431 cells protrude large spike-like filopodia that can be easily observed under a microscope. We used this simple assay system to identify compounds from microbial sources that inhibited filopodia protrusion.

After screening over 3000 microbial broth samples, we found that one broth from *Lechevalieria sp.* strain 1869-19 strongly inhibited EGF-induced filopodia protrusion in A431 cells (see Figure S1A available online).

To isolate the potential inhibitors in this broth, the broth extracts was separated into six fractions, numbered **I–VI**, by silica-gel chromatography with chloroform-methanol elution. However, no single fraction showed inhibitory activity against filopodia protrusion (Figure S1B). To examine whether the active substance may have degraded during chromatography, all six fractions were remixed (recombined fractions were termed "Remix") and tested for inhibitory activity. The Remix inhibited EGF-induced filopodia protrusion in the same concentration range as the broth extract (Figure S1C). These results suggested that the inhibition of EGF-induced filopodia protrusion was due to the synergistic action of two (or more) substances in the broth extract, and that these "active" substances were separated into different fractions during silica gel chromatography.

To determine which of the six fractions contained each active substance, we prepared remixes with one fraction withdrawn and assessed each such remix for ability or inability to inhibit filopodia protrusion. Withdrawal of fractions **I** (eluted from silica gel column by 100:0 chloroform:methanol) and **IV** (eluted by 100:5 chloroform:methanol) from the Remix resulted in no inhibition of filopodia protrusion (Table 1; Figure S1D), indicating that fractions **I** and **IV** contained active substances. Furthermore, combining fractions **I** and **IV** restored the inhibitory activity to a level comparable to the complete Remix, indicating that the mixture of the active substances in fractions **I** and **IV** was sufficient for inhibition of EGF-induced filopodia protrusion.

To identify the active substances in fractions **I** and **IV**, further isolation processes were undertaken. Fraction **IV** was subjected to silica gel column chromatography with toluene-acetone elution. Each resulting fraction was assessed for its ability to inhibit filopodia protrusion in the presence of fraction **I**. Fractions eluted with a toluene-acetone mixture at a 3:1 ratio demonstrated inhibition in the presence of fraction **I**, but not in its absence. Fractions showing the filopodia inhibition were collected and further purified by centrifugal liquid-liquid partition chromatography (CPC) using chloroform-methanol-water (5:4:6, ascending mode) elution, yielding a colorless, amorphous product. Analysis of MS and NMR spectra identified the product as glucopiericidin A (GPA) (Matsumoto et al., 1987) (Figure 1A).

The active substance in fraction **I** was purified by CPC using hexane-ethyl acetate-acetonitrile (5:1:4, ascending mode) elution, yielding pure yellow oil. This product was identified by MS